Numerical Simulation of the Indian Monsoon Climate using the WRF Regional Climate Model

Singuru MadhuSai
Department of Meteorology and Oceanography, Andhra University
Roshmitha Panda
Department of Meteorology and Oceanography, Andhra University
Surireddi Satya Venkata Sivaramakrishna (ssvs_rk@yahoo.co.in)
Department of Meteorology and Oceanography, Andhra University

Research Article

Keywords: SA-CORDEX, WRF, CMIP5, Regional climate Model, TTG

Posted Date: July 7th, 2023

DOI: https://doi.org/10.21203/rs.3.rs-3101084/v1

Abstract

Climate studies are essential in understanding the Earth's climate system and its dynamics. Numerical models play a significant role in these studies by simulating the behaviour of the atmosphere and providing insights into future climate scenarios. In the recent years, the Weather Research and Forecasting (WRF) model has emerged as a widely used tool for studying climate on regional scales. In the present study, we simulated the mean features of the Indian summer monsoon (June through September) climate using the WRF regional climate model. The WRF model with a horizontal resolution of 25 km is driven by the Community Climate System Model version4 (CCSM4) for the period 2006-2021 which is a part of the fifth generation of Coupled Model Inter comparison Project (CMIP5) using the Representative Concentration Pathway 6.0 (RCP6.0) over the South Asia Coordinated Regional Downscaling Experiment (SA-CORDEX) domain. The model is simulated on a continuous mode throughout its annual cycle for the period of integration. But for the presentation of results, the summer monsoon months of JJAS for the period 2007 to 2021 are only analysed. The performance of the model was assessed through the study of the spatial distribution of Air temperature (2m), Winds, Pressure, Rainfall, and the Vertical Integrated Moisture flux convergence (VIMFC). The simulated parameters were compared to those in ERA5 reanalysis and the India Meteorological Department (IMD) gridded rainfall. The performance of the WRF model was evaluated for simulating the regional scale precipitation over 5 homogenous rainfall zones of India. The WRF model accurately reproduces the Tropospheric Temperature Gradient (TTG) between the southern and northern regions. The sub-regional scale analysis of the simulated 2m temperature and precipitation for 30 meteorological subdivisions of India reveals that the WRF model performs better than the CCSM4 model. Results indicate that the model is able to capture the mean climatological features of the monsoon viz. monsoon onset, low-level Jet and the upper-level tropical easterly jet.

1. Introduction

An extensive knowledge of the climate change is very essential for scientists and policy makers since it is very crucial and has a very high impact on agriculture, health and water resources and the associated dynamics (Parthasarathy et al. 1994; Guhathakurta and Rajeevan 2008; Ghosh et al. 2016; Rai et al. 2018; Kumar et al. 2020; Katzenberger et al. 2021). Hence, there is a high sense of necessity for generating future climate scenario data for climate predictions. The variability of climate is studied on different scales such as inter annual, inter decadal and climate cycles. Normally, a climate cycle is considered for a period of 30 years (Schneider and Dickinson, 1974). Presently, coupled global climate models are being used to simulate future climate but these global models have a constraint on model resolution due to a huge demand of high speed computational resources. Hence to study the climate and its variability on a finer scale, we need to resort to regional climate models.

The Indian summer monsoon has been experiencing a sea change in its climate since 1995 Majra and Gur (2009). Since 1980’s several studies were in vogue for simulating regional climate; Giorgi (2019) presents an extensive review on regional climate modelling and a similar review has been given by Dash

et al. (2017) for regional climate studies over the Indian Subcontinent. The state of the art for studying regional climate is called dynamical downscaling which refers to the use of regional climate models to dynamically simulate the effects of large scale climate processes downscaled to regional scales. This technique of dynamical downscaling from global models to regional climate models was first introduced by Dickinson et al. 1989, and Giorgi and Bates, 1989.

Regional climate model studies have been successfully performed and adapted for various regions of the world mainly for the domains promoted by the CORDEX program. Many studies have been made for these CORDEX domains viz. South America (Chou et al. 2000, Menendez et al. 2001, Nobre et al. 2001, Nicolini et al. 2002,, Misra et al. 2002b & 2003, Seth and Rojas,2003 and Rojas and Seth,2003, Falco et al. 2019, Gomes et al. 2022), Central America (Cavazos et al. 2019, Cabos et al. 2019, Rivera et al. 2022),North America (Caya and Laprise,1999; Plummer et al. 2006; Caldwell et al. 2009; Meyer and Jin 2017; Martynov et al. 2013, Prein et al. 2019, Bukovsky et al. 2020), Europe (Christensen et al. 1997; Giorgi 1990; Jones et al. 1995,1997; Machenhauer et al. 1998; Heikkila et al. 2011; Dasari et al. 2014; Nastos and Kapsomenakis, 2015; Warscher et al. 2019; Jacob et al. 2020, Vautard et al. 2021, Outten and Sobolowski,2021), Africa (Hernández-Díaz et al. 2013; Laprise et al. 2013; Ayugi et al. 2020; Demissie and Sime,2021), East Asia (Kida et al. 1991; Hirakuchi and Giorgi 1995; Gao et al. 2015; Raghavan et al. 2016; Zou et al. 2016; Ratna et al. 2017; Afrizal and Surussavadee 2018; Gu et al. 2018; Kim et al. 2021), Central Asia (Öztürk et al. 2012; Qiu et al. 2017; Russo et al. 2019; Rai et al. 2022), Australasia (Wamahiu et al. 2020; Evans et al. 2021; Nishant et al. 2021; Turp et al. 2022), Antarctica (Souverijns et al. 2019; Bozkurt et al. 2020, 2021; Carter et al. 2022), Arctic (Berg et al. 2013; Glisan et al. 2014; Koenigk et al. 2015; Takhsha et al. 2018), South East Asia (Chotamonsak et al. 2011; Tangang et al. 2019,2020). Apart from the above studies, many studies have been made for the SA-CORDEX domain especially for the Indian sub-continent (Maharana and Dimiri,2014; Karmacharya et al. 2015; Raju PVS et al. 2015; Iqbal et al. 2017; Maity et al. 2017; Choudhary et al. 2018; Pattnayak et al. 2018; Maurya et al. 2018; Rana et al. 2020; Singh et al. 2021; Tyagi et al. 2022; Ramakrishna et.al. 2022; Barde V et al. 2023).

Polanski et al. 2010 used a regional climate model HIRAM to investigate the Indian summer monsoon for the period 1958–2001 at a horizontal resolution of 50km with the initial and lateral boundary conditions taken from ERA40 reanalysis data. Kumar et al. 2011examined the impact of global warming on the Indian monsoon climate using Hadley Centre's high resolution regional climate model, PRECIS (Providing REgional Climates for Impact Studies). The simulations correspond to the Intergovernmental Panel on Climate Change (IPCC) Special Report on Emissions Scenarios (SRES)-A1B emission scenario and are carried out for a continuous period of 1961–2098. Mathison et al. 2012 performed four regional climate model simulations with the HighNoon regional climate model for India and Himalaya at a resolution of 25km from 1960 to 2100 to provide an ensemble of simulations for the region. Saeed et al. 2012 proposed an evaluation framework for the better assessment of the capability of an RCM in capturing the fundamental structure of South Asian Summer Monsoon (SASM), because the regional climate model (RCM) deals with only few variables which is insufficient for the validation. To achieve this, the framework has been applied to the regional climate model REMO using ERA40 as boundary conditions for the period 1961–2000. Maharana and Dimri, 2014 studied the climatology and the inter annual

variability of basic meteorological fields over India and its six homogeneous monsoon sub regions by using the Regional Climate Model Version 3 (RegCM3) for the period 1980–2001 with the initial and lateral boundary conditions taken from NNRP2. Dasari et al. 2014 performed regional climate simulations of the Europe for a period of 60 years (1950–2010) by using the WRF model at a resolution of 25km. The model is forced with NCEP 2.5 degree reanalysis as initial and lateral boundary conditions. Syed et al. 2014 performed simulations using two regional climate models RegCM4 and PRECIS over South-Asia by downscaling the global data of ERA40 reanalysis and ECHAM5 general circulation model for the summer monsoon in order to estimate the uncertainties of the RCMs in reproducing the present-day climate (1971–2000). Niu et al. 2015 studied the Indian monsoon climate for the control climate period 1981–2000 obtained from three global climate models (GCMs) and seven regional climate models (RCMs). Halder et al. 2016 studied the role of Land Use Land Cover (LULC) on the Indian summer monsoon rainfall and temperature using a regional climate model (RegCM4.0) for the period 1951–2005. Two sets of model simulations were performed each for 27 years with similar lateral boundary conditions (LBCs) from NCEP/NCAR reanalysis and Reynolds weekly SST prescribed at the lower boundary, but different land cover for the years 1950 and 2005 as fixed lower boundary condition. Karmacharya et al. 2015 carried out three experiments to understand the influence of domain size and shape on the inherent model biases; i.e., with GCM simulation, with nudged GCM simulation and with RCM simulations over four different domains. Gao et al. 2017 investigated the relative role of the land surface schemes and forcing datasets in the Dynamical Downscaling Modelling (DDM) over the Tibet Plateau (TP), a region complex in topography and vulnerable to climate change. Three simulations with two land surface schemes were performed using the WRF model at 30km resolution for the period 1980–2005. Two simulations were forced by the ERA-Interim reanalysis dataset and the other simulation was forced by a GCM-CCSM. Iqbal et al. 2017 conducted a number of simulations with the fourth release of the Rossby Center Regional Climate Model (RCA4) within the SA-CORDEX at 50 km horizontal resolution which are evaluated for mean summer (June–September) and winter (December–March) climate for the period 1980–2005. Choudhary et al. 2018 assessed the performance of 11 regional climate simulations of SA-CORDEX in representing the precipitation patterns of summer monsoon over India for the period 1970–2005. Pattnayak et al. 2018 assessed the performance of two versions of RegCM models (V4.2&V4.3) by simulating the Indian summer over the South Asia for the period 1998–2003 with an aim of conducting future climate change simulations. Fonseca and Martin-Torres,2019 simulated the climate of the Kerguelen Islands by using the WRF model at a horizontal resolution of 3km for the period April 1986-March 2016.

Huo and Peltier,2020 investigated the South Asian Monsoon using the WRF model at a horizontal resolution of 10km over Indian sub-continent for the period 1980-94. Rana et al. 2020 investigated the model errors and the projected climate change in seasonal mean temperature and precipitation over South Asia by using two ensembles of climate simulations; one global and one regional. The regional climate model RCA4 is simulated by downscaling the global ensemble (includes 10 global climate models) and the regional ensemble (all 10 GCMs) over South Asia at 50km resolution for the period 1981–2010. Ramakrishna et al. 2022 studied the climate of India by generating the regional climate data

using the WRF model at 25km horizontal resolution for the period 1976–2005 using CMIP5-CCSM4 as a forcing data. The model simulated outputs were categorized for four seasons and are compared to the observational datasets. The results indicate that the simulated pre-monsoon heating and post-monsoon cooling over the land is in good agreement with the analysis and that the simulated rainfall over central and south peninsular India during south west monsoon season is well distributed. This validated data would be useful for identifying the climate change on regional scales and also useful for agriculture and water vapour availability for future climate studies.

Barde et al. 2023 examined the projected changes in the Indian Summer Monsoon Region (ISMR) over East India (EI) with two emission scenarios, RCP4.5 and RCP8.5, for near (2017–2040) and far-future (2041–2070) projections using a set of ten CORDEX-SA Regional Climate Model (RCMs). The above information reveals that out of 19 studies, 14 were done for climate simulation over India. Out of the 14 done for India, 10 studies were for the Indian monsoon season.

For the present study, WRF (ARW) model has been used to derive the regional climate data pertaining to future climate simulations with RCP6.0 scenario. The rationale for choosing the RCP6.0 is due to its middle of the ground approach to future changes in radiative forcing. In RCP6.0, total radiative forcing is stabilised at 6.0 W/m2 after 2100 by utilising a variety of technologies and strategies for reducing greenhouse gas emissions. This is accomplished by time series of emissions and concentrations of the full suite of greenhouse gases, aerosols, chemically active gases, as well as land use/land cover. This study forms a part of the project sponsored by the Govt. of India, Department of Science and Technology (DST) under the aegis of National Mission on Strategic knowledge for Climate Change (NMSKCC).The very purpose of this study is to derive the future climate projections and the advantages of the regional climate model from a general circulation model. The present study is motivated to evaluate the performance of the WRF model in deriving the regional scale features using the currently possible 15 year simulations of 2007–2021. This evaluation is a possible indicator of the assumed greenhouse emissions and the formulation of model physics. The future climate projections that are generated and validated have many applications in sectors like agriculture, health, water resources and climate change adaptations. The present paper is divided into 5 sections. Section 1 is on introduction, section 2 gives the details of the CCSM4 and the WRF models. Section 3 describes the data and methodology adapted for the present study, section 4 presents the results, and section 5 summarizes the results.

2. Description of the Models

CCSM4 Model:

The CCSM4 model was developed and maintained by the National Center for Atmospheric Research (NCAR, US) which is a coupled general circulation model consists of four components i.e., atmosphere, land, ocean and sea-ice through a central coupler component that exchanges state information and fluxes between the components (Gent et al. 2011). The CCSM is one of the climate models included in the World Climate Research Program's (WCRP's) CMIP5 (Taylor et al. 2012). The CCSM4 is a subset of

Community Earth System Model (CESM1). The CESM1 is a coupled global climate model that provides state of the art computer simulations of the Earth's past, present, and future climate states. The CCSM4 uses CAM4 model for the simulation of the atmospheric component. The detailed information of the model configuration is described in Appendix. The CCSM has been widely used in studying several paleoclimate epochs, the climate of the more recent past, and to make projections of future climate change (Gao et al. 2017). CCSM4 uses the conventional approach in the form of shallow and deep convection parameterization (Neale et al. 2013). The detailed information regarding the model and the availability of data is in https://www.cesm.ucar.edu/models/ccsm4.0/ website. Several climate studies have been done using the CCSM4 model data (Cook et al. 2012; Islam et al. 2013; Ma et al. 2015; Meyer and Jin 2016; Stan and Xu 2015; Gao et al. 2017; Ramakrishna et al. 2022).

WRF Model:

The WRF model used here for the regional climate simulations is a state of the art model developed by NCAR which is a mesoscale numerical weather prediction system designed for both atmospheric research and operational forecasting applications. It is a non-hydrostatic mesoscale model that uses terrain following hybrid sigma-pressure vertical coordinate system available with several advanced physics and numerical schemes, designed for better prediction of atmospheric processes. Further details of the WRF model can be found at Skamarock et al. (2008). Several climate studies were done using the WRF model (Dasari et al. 2014; Meyer and Jin, 2015; Raghavan et al. 2016; Abdelwares et al. 2018; Fonseca and Martín-Torres, 2019).

3. Data and Methodology

Datasets used

The CCSM4 model is used to drive the boundary conditions for the WRF model. The atmospheric and the ocean surface temperature data needed for generating the initial and boundary conditions for simulations are provided in a single bias corrected datasets of CCSM4, which are available in the Intermediate file format specific for WRF/MPAS in the website (https://rda.ucar.edu/datasets/ds316.1/) (Bruyere et al. 2015). These datasets include a historical simulation and three future projections. A 20th century simulation (“20THC”) was forced by observed natural and anthropogenic atmospheric composition changes spanning 1951–2005 and the future projections are generated under RCPs 4.5, 6.0 and 8.5 (Moss et al. 2010), spanning 2006–2100. The data provided at a horizontal resolution of 1.25^0 latitude x 0.9^0 longitude and are interpolated to 26 pressure levels at every 6-h regular intervals is used for the present study.

The fifth-generation European Center for Medium-Range Weather Forecast (ECMWF) ERA5 reanalysis (Copernicus Climate Change Service, 2017) was used for the validation of the atmospheric variables. The ERA5 dataset provides hourly estimates for a large number of atmospheric, ocean-wave and land-surface quantities globally at a horizontal resolution of 0.25° x 0.25° (atmosphere), 0.5° x 0.5° (ocean waves).

The data has been regridded to a regular lat-lon grid. For the validation of rainfall, daily gridded precipitation dataset over the Indian landmass from the India Meteorological Department (IMD) providing New High Spatial Resolution at 0.25^0 X 0.25^0 (Pai et al. 2014) is used. This new gridded dataset is prepared by collecting daily rainfall records from 6955 rainfall gauge stations (highest number of stations) in India. This dataset is available in millimetres (mm) for 122 years (the long period 1901–2022) arranged in 135x129 grid points and can be accessed through https://www.imdpune.gov.in/cmpg/Griddata/Rainfall_25_NetCDF.html. The daily gridded maximum and minimum temperature dataset from IMD at a resolution of 1^0 X 1^0 is used (Srivastava et al. 2009) to perform the statistical metrics for sub divisions.

Methodology

Regional climate model simulations for the period 2006–2021 using the WRF model are presented in this study. The rationale for choosing the period is that we have simulated the climate from the period when the RCP 6.0 scenarios corresponding to the CCSM4 have been ingested. The simulation has been performed using Advanced Research WRF model version 3.9 (Skamarock et al. 2008) over the SA-CORDEX domain covering 15.5^0 E – 116.5^0 E and 16.5^0 S- 47.5^0 N with 389 grid points in the east-west direction and 274 grid points in the north-south directions (Fig. 1). The physics included the WSM6 microphysics, BMJ for cumulus convection (Betts and Miller 1986), (Janjic 2000), RRTMG for both shortwave and long wave radiation processes (Iacono et al. 2008) and the Yonsei University scheme (YSU) for the Planetary Boundary Layer (PBL) turbulence (Hong et al. 2006). Detailed information is presented in the Table1.

In an earlier study, the WRF model at 25km horizontal resolution was integrated for the period 1971–2005 using CMIP5-CCSM4 data (Ramakrishna et al. 2022). In the present study, the model is forced with the CMIP5-CCSM4 RCP6.0 boundary conditions for the period 2006–2021. The model integrations were carried out from 1st January 2006 up to 31st December 2021 for a continuous period in a climate mode. But for the analysis, we chose the summer monsoon (JJAS) season only for the period 2007 to 2021 considering 2006 as spin-up-time. The regional climate simulations are expected to simulate finer features compared to the CCSM4 global climate model which is used as the forcing to the WRF regional climate model. The WRF regional climate model results are validated in terms of the simulated atmospheric variables of 2m air temperature, Mean Sea level Pressure and Winds in comparison with ERA5 reanalysis dataset and rainfall with IMD gridded dataset. To assess the evolution of summer monsoon, the latitude-pressure cross section of vertical velocity (ω)(Kumar et al. 2020) and the Vertically Integrated Moisture Flux Convergence (VIMFC) (integrated over 1000 to 300hPa) (Fasullo and Webster.2003 and Ramakrishna et.al 2017) have been computed.

The equation for VIMFC is as follows

$$\mathrm{VIMFC} = -\frac{1}{g}\int_{1000}^{300}\left(\frac{\partial uq}{\partial x}+\frac{\partial vq}{\partial x}\right)dp$$

where ‘g’ is the acceleration due to gravity, ‘u’ and ‘v’ are zonal and meridional components of wind, ‘q’ is specific humidity, ‘p’ represents the pressure.

Further, to investigate the intensity of the monsoon circulation and the gradient between land and sea, the Tropospheric Temperature Gradient (TTG) is calculated between the southern (15^0 S-5^0 N, 40^0 E-100^0 E) and the northern (5^0 N-35^0 N, 40^0 E-100^0 E) regions during JJAS and presented. The evaluation of the model simulated rainfall is validated with the IMD gridded data by performing the statistical metrics for only five homogenous regions of India by excluding the hilly regions. The homogeneous regions are considered following Parthasarathy et al (1995). In order to illustrate the meridional variations adequately to the south and north of the monsoon trough, the zonal wind cross-section and meridional distribution of temperature were generated along the 78^0E longitude, which roughly passes through the median. In addition the evaluation of model simulated surface temperature and rainfall is done at sub divisional scale by performing the statistical metrics (i.e.) mean and standard deviation. The IMD uses 36 subdivisions for operational forecasts out of which only 30 subdivisions were used for the evaluation after excluding the hilly regions and the Islands in the Bay of Bengal and Arabian Sea. The temperature and rainfall for each subdivision from the grid point values has been computed by taking the area average of the corresponding subdivision.

4. Results and Discussion

The months of June, July, August and September comprise of the summer monsoon season which is the most important period for the Indian Sub-continent from a view point of agriculture and water management. The monsoon gets generated due to the differential heating of the Indian sub-continent and the North Indian Ocean. The model simulations for the Indian sub-continent would be termed as good if they can reproduce the primary features of the Indian summer monsoon namely, the heat low over the north western parts of India, the axis of the monsoon trough, the low level jet over the south peninsula and the Tropical Easterly Jet near to 10^0 N.

4.1. Spatial distributions:

In the following, the seasonal (JJAS) mean spatial distributions of 2m air temperature, mean sea level pressure (MSLP), wind at 850 hPa and 200 hPa and surface rainfall are presented and the salient features only are portrayed.

4.1.1.2m air temperatures: The spatial distributions of mean 2m air temperature (^{0}K) simulated by the WRF model and the CCSM4 model and ERA5 reanalysis are presented (Fig.2 a,b,c). The difference between WRF and ERA5, which indicate model bias are presented in (Fig.2d.) and the difference of the

mean 2m air temperatures between the two periods of (2007-2021)and(1976-2005) for the WRF model and ERA5 reanalysis are presented in (Fig.2e and 2f). The temperature minima over the Himalayan and the Tibetan plateau region are well reproduced. The WRF model simulated temperatures show higher values over the northwest part of the Indian sub-continent in comparison to the temperatures of CCSM4 and ERA5. The model also shows higher values in the northern parts of India and slightly lower values over Kerala and parts of Karnataka compared to the CCSM4 but with higher values over the Western Ghats compared to the ERA5 reanalysis. This slight variation may be attributed to the differences in the representation of orography of the Western Ghats in the WRF and CCSM4 models. The meridional gradient of the temperature is more in the WRF model as compared to the CCSM4 and ERA5. The model simulated surface temperatures are similar to those in the CCSM4 while in the ERA5 analysis they show slightly lesser temperatures over the Western Ghats. The bias for the surface temperature (WRF-ERA) shows positive bias over Rajasthan and parts of Uttar Pradesh while it shows negative bias over Tamil Nadu, Kerala and western part of the Himalayan region. From the figures (2e and 2f) a strong warm tendency of 0.5^0 K is observed over Indian landmass region in ERA5 analysis whereas in the WRF model a warm tendency of 0.25^0K is observed in most parts of India except Central India which indicates underestimation of temperatures over that region by the WRF Model. Further the deviation is higher over central India which is generally hotter than the southern parts. This underestimation of the temperatures may be attributed to the adopted physical parameterization schemes in the WRF model.

4.1.2. Mean Sea Level Pressure (MSLP): The spatial distributions of MSLP (hPa) simulated by the WRF model and the CCSM4 model and ERA5 reanalysis are presented (Fig.3 a,b,c). The difference between WRF and ERA5, which indicate model bias are presented in Fig.3d. and the difference of the MSLP between the two periods of (2007-2021) and (1976-2005) with the WRF model and ERA reanalysis are presented in Fig.3e and 3f. The model simulated MSLP is in good agreement with CCSM4 simulation and ERA5 analysis but the WRF model shows strong pressure gradients between northern parts of India and southern parts of India, which correspond to higher temperature gradients over the same region. The observed lowest pressure over the Northwest India is around 1000hPa in WRF, CCSM4 and ERA5 analyses whereas this area of lowest pressure extends up to the eastern parts of India in the WRF Model. The extent of the monsoon trough is better simulated in the WRF model where the negative bias could be seen right from the Northwest parts up to the Northeast parts of India (Fig.3d). The figure (3e, f) depicts the MSLP anomalies for the WRF and ERA5. The strong positive pressure tendency is observed over North-India, Northeast India and weak positive pressure tendency is observed over Tamil Nadu in ERA5 analysis whereas in the WRF model the weak positive pressure tendency is observed over South Peninsular India only.

4.1.3. Wind flow at 850 hPa and 200 hPa:

The wind flow at 850hPa level (Fig.4 a,b,c) shows similar patterns between CCSM4 and ERA5, while the WRF model simulated winds show a slightly weaker magnitude winds over the Arabian Sea and higher over the Bay of Bengal. The monsoon westerlies and the monsoon trough are very well simulated by the WRF model. The WRF model simulated stronger westerlies over the Bay of Bengal as compared to the

CCSM4 and ERA5. A stronger cyclonic flow in the vicinity of the monsoon trough region can be clearly seen as compared to that in the CCSM4 and ERA5 analysis. The figure 4 d and 4e depicts the wind anomalies for the ERA5 and WRF model. A strong positive tendency of magnitude (0.75 to 1 m/s) is observed over the Arabian Sea extending up to the Bay of Bengal in WRF model whereas a weak positive tendency is limited to the southwest part of the Arabian Sea as observed in the ERA5 analysis. A strong negative tendency is observed over the Northwest (Gujarat and Rajasthan States) and Central India regions in ERA5 analysis whereas a weak negative tendency is observed in the WRF model with a lesser magnitude of 0.5 (m/s).The WRF simulated 200hPa winds (not shown) are in good agreement with CCSM and ERA analysis, while the WRF simulated higher winds around 0 to 5^0 N. The anti-cyclonic flow around 27^0 N in WRF model is slightly less with a magnitude of 6 m/s when compared to CCSM4 and ERA5. The easterlies around 10^0 N are well simulated, in correspondence with CCSM4 and ERA5.

4.1.4. Rainfall: The spatial distribution of rainfall of the CCSM, WRF model and IMD gridded rainfall are depicted in figure 5 (a, b, c). The model simulated rainfall over the Northern part of India shows good correspondence with CCSM and IMD rainfall. The WRF model is able to capture the spatial patterns of the precipitation over Central India and Northeast regions with higher magnitudes and West coast region with lesser magnitudes as compared to the IMD rainfall. The maximum amount of rainfall during the summer monsoon is due to the convection generated in the region of Monsoon trough and its adjoining low pressure areas. The deviation of rainfall between IMD and WRF over the west coast region may be due to the hilly terrain in that region. From the figure 5d which shows the bias of mean rainfall of the period 2007-2021 for the monsoon season that a positive bias (higher rainfall) over the central India and northeast parts of India and a negative bias (lower rainfall) over the west coast, northwest and northern parts of India are noted. The figure 5(e, f) represents the rainfall anomalies of WRF and IMD for the periods (2007-2021) minus (1976-2005). A positive tendency is observed over the Western Ghats and central parts of India in the WRF model whereas in the IMD rainfall the positive tendency is observed in some parts of Western Ghats and in Gujarat. This may be attributed to a changing climate in the global warming era.

4.1.5. Vertical Integrated Moisture Flux Convergence: The VIMFC along with its transport is calculated in Fig.6(a-c) to investigate the transport of moisture towards the Indian landmass region of CCSM4, WRF and ERA5. The VIMFC is calculated by integrating vertically the horizontal moisture flux convergence/divergence between the surface and 300 hPa. The negative values indicate the convergence and the positive values indicate the divergence. It is evident that there is a moisture convergence along the coast of Somalia and the northern part of the Arabian Sea and that the moisture is transported from the Arabian Sea to the Indian landmass region in CCSM4, WRF and ERA5. There is a strong convergence over the west coast and northeast parts of India as observed in the WRF model compared to the CCSM and ERA which is in good correspondence to the rainfall over those regions. Also the WRF model had simulated the cyclonic circulation very well over the Head Bay of Bengal region which is in good agreement with CCSM4 and ERA5 analysis.

4.2. Rainfall in homogenous regions:

The evaluation of rainfall in the different homogenous regions has been made from a view point of statistical metrics (i.e.) Mean, Standard deviation, Root mean square error and correlation coefficients (CC). As a part of the evaluation, six homogenous regions (Fig.7) are considered as mentioned earlier Parthasarathy et al. 1995. Among the 6 homogeneous regions, the various statistical metrics have been calculated for 5 homogenous regions after excluding the hilly regions and for All India are presented in Table 2. The CC values are higher in all the homogenous regions 0.8 and above. The CC for All India is 0.6. The correlation is highest in the Central North East region which is the area of convergence of the Monsoon Trough. The RMSE shows minimum value in the South Peninsular region where there is usually substantial rainfall especially during the Monsoon onset. The maximum Mean and standard deviation values are observed over the West-Central region in both the WRF and IMD. The various statistical metrics show that the model could simulate the characteristics of the monsoon rainfall.

4.3.1 Tropospheric temperature gradient

Fig.8 shows TTG from the WRF model and ERA analysis. The temperature gradient between Southern and Northern regions averaged over 600-200hPa is defined as the TTG. The TTG characterizes the strength, onset and withdrawal of the Indian Summer Monsoon. For accessing the intensity of the model simulated land-sea gradient, the temperature difference between South (15^0S-5^0 N, 40^0E-100^0E) and North (5^0 N-35^0 N, 40^0E-100^0E) regions of the Indian sub-continent is analysed and presented. The blue line indicates the ERA analysis and red line indicates the WRF model simulation. The WRF model very well simulated the structure of the Tropospheric temperature gradient throughout its annual cycle. This can be attributed to the fact that the southern region contains more ocean than the northern region and that in the pre-monsoon season the temperature between land and sea would be more which gradually decreases once the monsoon sets in. The model TTG is in perfect agreement with the ERA5 analysis which indicates the good simulation of temperature distribution over the Indian sub-continent.

4.3.2. Meridional distribution of temperature: Fig.9 (a-c) depicts the time-latitude sections of the monthly mean temperatures at 850 hPa level along 78^0 E. From the figures, it is clearly observed that there is a gradual increase of temperatures from lower latitudes to higher latitudes with a maximum during April-June. The maximum temperature is observed between 20^0N to 26^0 N in CCSM whereas the maximum is observed between 18^0N to 30^0 N in WRF model. The WRF model is slightly overestimated the temperatures compared to ERA analysis.

4.3.3.Zonal wind cross-section: Fig.10(a-d) shows the latitude-height cross section of the zonal winds along 78^0 E for pre-monsoon and monsoon Season. The WRF model simulated the patterns both for pre-monsoon and monsoon season well which are in good correspondence with ERA5 analysis. The strong westerlies in the upper troposphere are observed at 22^0N to 30^0 N and slightly strong easterlies are observed at lower latitudes in WRF model compared to ERA during pre-monsoon season. During the monsoon season, the strong westerlies are observed in the lower troposphere and stronger easterlies in upper troposphere at a level of nearly 200hPa during monsoon season which are in good agreement with

ERA5 but with slight stronger magnitudes. The strong westerlies in the upper troposphere are observed over middle latitudes in the WRF which are consistent with ERA5.

4.3.4. Vertical velocity distribution: The latitude-pressure profile of vertical velocity (ω) has been analysed to observe the vertical motion of atmosphere and is presented in Fig.11 (a, b). The vertical motion in the atmosphere plays a key role in the transfer of mass and energy leading to the formation of clouds which affects the atmospheric stability. From the figure, the positive values signify sinking and negative values signify rising motion. A strong rising motion in the WRF is observed at around 27^0 N and a weak rising motion has been seen over 10^0 N-20^0 N which is in agreement with ERA. A rising branch indicates an active convection over that region.

4.4. 1 Sub-divisional evaluation of temperatures for the pre-monsoon

In the pre-monsoon season, weather over the Indian sub-continent largely defines the performance of the ensuing monsoon since monsoon is a magnificent heat engine that evolves due to the differential heating between land and sea. An evaluation of temperature simulation is performed in terms of Mean and Standard deviation for the subdivisions (fig 12) during the pre-monsoon season. The statistical metrics are shown for 30 sub divisions in table 3. From the results, it can be seen that the WRF model simulates the better mean values of temperatures over 20 sub divisions whereas standard deviation is over 22 sub divisions better than CCSM4. The pre-monsoon temperatures are very important since much of the moisture inflow will be there from the adjoining ocean to the main land. The gradient between the land and the ocean facilitates the advection of moisture from the ocean to the land. The pre-monsoon heating of the land helps the building of vertical velocities and thereby leading to rainfall during the monsoon season. A good simulation in terms of the statistical metrics implies a better prediction of sub regional scale temperatures by the model.

4.4.2 Sub-divisional evaluation of surface temperature and rainfall during monsoon season

The evaluation of model simulated surface temperature and rainfall is performed by calculating the Mean and Standard deviation for the monsoon period in the sub divisions (Fig.12) of Indian sub-continent with IMD gridded data and CCSM4 data. Tables 4 and 5 represent the statistical metrics for temperature at 2m and rainfall respectively.

The WRF model had simulated the mean temperatures better than CCSM4 for 22 subdivisions and a positive bias is observed over Northern and Central parts of India compared to IMD and CCSM4. The WRF model had shown the higher standard deviation values than CCSM4 in most of the subdivisions. The magnitudes of standard deviation range from 0.5 to 2.1 for IMD whereas the values range from 0.5 to 3.5 in WRF model.

A good amount of rainfall is observed during the monsoon season with 24 sub divisions yielding rainfall higher than 5mm/day. The highest amount of rainfall is received over Konkan& Goa (25.7 mm/day) and Coastal Karnataka (22.9 mm/day) and the lowest rainfall is over West Rajasthan (2.6 mm/day) and

Tamil Nadu (3.3 mm/day. The model had produced better mean values of rainfall over 20 sub divisions and better standard deviation values of rainfall over 14 sub divisions compared to the rainfall simulated by CCSM4.

The above presentation of the results simulated by the WRF model run on a climate mode clearly demonstrates the advantage of using a WRF model on a finer resolution to simulate future climate.

5. Summary and Conclusions

Future projections of the Regional Climate data is essential to understand the climate change on regional scales have been generated using the WRF model at 25 km resolution on a climate mode for the South Asian CORDEX domain. The WRF model is forced with the CCSM-4 global coupled model for the future period of 2006 to 2021.Seasonal averages for the monsoon period are evaluated in terms of wind, pressure, temperature and rainfall in comparison to the ERA global reanalyses and the gridded rainfall provided by the India Meteorological Department. The RCP 6.0 scenario follows the prescribed values of CO2 emissions in a projected climate scenario. These levels of greenhouse gases will increase the temperatures and also gives us an estimated temperature rise. The WRF having a finer resolution (25km) has the capability of predicting higher temperatures on a finer resolution when compared to CCSM4 with a coarser resolution (~100km).

The following are the important results obtained through this study:

The WRF model had simulated the spatial distribution of temperature well which is in good agreement with observations but with a slight overestimation over northern and central parts of India. The model simulated pressure shows strong pressure gradients between northern and southern parts of India, which is in good agreement with higher temperature gradients over the same region. The model had simulated the low-level westerly wind flow over the Arabian Sea and Bay of Bengal and is in agreement with observations but with a weaker magnitude over the Arabian sea and stronger over the Bay of Bengal. The model had produced the monsoon trough accurately which extends from the northern parts to the head Bay of Bengal. The monsoon trough plays a crucial role in the summer monsoon precipitation as the maximum amount of rainfall during this season is obtained due to the convection generated in the trough region and its adjoining low pressure areas. An anti-cyclonic circulation over sub-tropical ridge at 30^0 N and the tropical easterly jet at 15^0 N are in good agreement with the observations. The WRF had simulated the spatial distribution patterns of higher rainfall over the Central India, North East India and patterns of lesser rainfall over the west coast of India which is in agreement with IMD but with higher magnitudes over the high rainfall region and lower magnitudes over the low rainfall region.

The analysis of the VIMFC shows the moisture convergence over the Somalia coast and the northern part of Arabian Sea and its transport from ocean to the Indian landmass region. Strong convergence is observed over the west coast of India that represents the monsoon precipitation over that region. The model had produced the cyclonic circulation over the Head Bay of Bengal well which is in agreement with

the ERA5 analysis. The latitude-pressure cross section of vertical velocity (ω) shows that the WRF model had produced the meridional circulation well. A strong vertical motion over the monsoon trough region with descent over equatorial regions depicts the reverse Hadley circulation as typical to the Indian Southwest Monsoon circulation.

The model had reproduced the TTG and the meridional temperature gradient well which is in good agreement with ERA5 analysis. The simulated meridional Tropospheric wind flow between pre-monsoon and monsoon season over the Indian sub-continent depicts all the characteristics of the pre-monsoon and monsoon seasons.

The WRF model had simulated the sub regional scale temperature and rainfall better than CCSM4 model. Our results suggests that the WRF model had reproduced most of the characteristics of Monsoon such as low-level cross equatorial flow over Somalia coast, westerlies over Arabian Sea, Monsoon trough, heat low over northwest, sub-tropical ridge, tropical easterly jet at upper levels and the monsoonal precipitation. All these features accentuate the model performance over the regional scale.

The results of differences in temperatures between the periods of 2007-2021 and 1976-2005 indicate a possible warming of ~0.25 K in 15 years, which is in good agreement with ERA and IMD analyses. This inference implies that the chosen greenhouse emissions generate the observed warming over India as a part of the current global warming trends since 1980s. However, it is not to be understood that RCP6.0 mimics the present warming trend as all the scenarios are expected to produce similar warming the first few decades before the greenhouse emission trends modulate the temperatures. The present evaluation supports the global model pattern future projections and the application of limited area such as WRF to infer regional scale features associated with the warming scenario.

The WRF model had produced the essential differences in the anomalies of 2m air temperature, MSLP, wind regimes and rainfall with the spatial distribution features agreeing with ERA5. These results make it favourable to infer that the RCP6.0 scenario leads to satisfactory evaluation of feature climate projections during the first 15 years. This inference is to be taken with a caution that a continuation of the tendencies has produced by the model may or may not correspond with the real evolution has the model future climate projections are strictly controlled by the forcing of the RCP6.0 global warming scenario.

The study would be continued by generating future climate data for the near future period up to 2050 and for the far future period 2051-2100.

Declarations

Acknowledgements: The authors acknowledge the advice of Prof. D.V. Bhaskar Rao, Honorary Professor and mentor of the DST sponsored project at the department of Meteorology and Oceanography, Andhra University and also we thank for the free availability of CCSM4 data, ECMWF for providing the ERA reanalyses data and the IMD for providing the gridded data. User support and a free access of the WRF model is acknowledged along with the GrADS software in which the plots are drawn.

Data availability: The data for driving the regional model has been obtained from NCEP-RDA and ERA data from ECMWF, Reading, England and the rainfall data from the India Meteorological Department, New Delhi, India.

Code availability: The WRF model code is obtained from NCAR/NCEP, USA

Authors' Contribution:

Singuru MadhuSai performed the WRF model experiments, analyses and visualization.

Roshmitha Panda contributed to the WRF model experiments and adaptation.

Surireddi Satya Venkata Sivaramakrishna contributed to the Model Design, experimentation and paper drafting.

Funding: The present work was done through a support grant from the Department of Science and Technology (DST) Government of India. The first author Mr S. Madhusai expresses his gratitude to the DST, Government of India for providing the fellowship in research project under NMSKCC (Ref No DST/CCP/MRDP-97/2017(G)).

Ethics approval: All the authors have read the manuscript and approved the manuscript.

Consent to participate: The authors have given their consent for submitting this paper to the Journal of Theoretical And Applied Climatology.

Consent for publication: The authors agree to give permission to the publisher to publish their work.

References

1. Abdelwares, M., Haggag, M., Wagdy, A., &Lelieveld, J. (2018) Customized framework of the WRF model for regional climate simulation over the Eastern NILE basin. Theoretical and Applied Climatology, 134, 1135–1151. https://doi.org/10.1007/s00704-017-2331-2.
2. Afrizal, T. &Surussavadee, C. (2018) High-Resolution Climate Simulations in the Tropics with Complex Terrain Employing the CESM/WRF Model. Advances in Meteorology, 1-15. https://doi.org/10. 1155/2018/5707819.
3. Ayugi, B., Tan, G., Ruoyun, N., Babaousmail, H., Ojara, M., Wido, H., Mumo, L., Ngoma, N.H., Nooni, I.K., Ongoma, V. (2020) Quantile Mapping Bias Correction on Rossby Centre Regional Climate Models for Precipitation Analysis over Kenya, East Africa. Water (Switzerland), 12, 801. https://doi.org/10.3390/w12030801.
4. Barde, V., Nageswararao, M.M., Mohanty, U.C., Panda, R.K. (2023) Performance of the CORDEX-SA Regional Climate Models in Simulating Summer Monsoon Rainfall and Future Projections over East India. Pure and Applied Geophysics.**180**, 1121–1142. https://doi.org/10.1007/s00024-022-03225-3.

5. Berg, P., Döscher, R., &Koenigk, T. (2013) Impacts of using spectral nudging on regional climate model RCA4 simulations of the Arctic, Geoscientific Model Development, 6, 849–859, https://doi.org/10.5194/gmd-6-849.
6. Betts AK, Miller MJ (1986) A new convective adjustment scheme. Part II: Single column tests using GATE wave, BOMEX, ATEX and arctic air-mass data sets. Q J R MeteorolSoc 112(473):693–709. https://doi.org/10.1002/qj.49711247308.
7. Bozkurt, D., Bromwich, D.H., Carrasco, J., Hines, K.M., Maureira, J.C., &Rondanelli, R. (2020) Recent Near-surface Temperature Trends in the Antarctic Peninsula from observed, reanalysis and Regional Climate Model Data.Advances in Atmospheric Sciences, 37(5), 477–493, https://doi.org/10.1007/s00376-020-9183-x.
8. Bozkurt, D., Bromwich, D.H., Carrasco, J., Rondanelli, R. (2021) Temperature and precipitation projections for the Antarctic Peninsula over the next two decades: contrasting global and regional climate model simulations. Climate Dynamics, 56, 3853-3874. https://doi.org/10.1007/s00382-021-05667-2.
9. Bruyere, C. L., Monaghan, A. J., Steinhoff, D. F., & Yates, D. (2015) Bias-Corrected CMIP5 CESM Data in WRF/MPAS Intermediate File Format (No.NCAR/TN-515+STR).doi:10.5065/D6445JJ7.
10. Bukovsky, M.S., Mearns, L.O. (2020) Regional climate change projections from NA-CORDEX and their relation to climate sensitivity. Climatic Change 162, 645-665. https://doi.org/10.1007/s10584-020-02835-x.
11. Cabos, W., Sein, D.V., Durán-Quesada, A., Liguori, G., Koldunov, N.V., Martínez-López, B., Alvarez, F., Sieck, K., Limareva, N., & Pinto, J.G. (2019) Dynamical downscaling of historical climate over CORDEX Central America domain with a regionally coupled atmosphere-ocean model. Climate Dynamics 52, 4305–4328.https://doi.org/10.1007/s00382-018-4381-2.
12. Caldwell, P., Chin, HN.S., Bader, D.C., Govindasamy, B. (2009) Evaluation of a WRF dynamical downscaling simulation over California. Climatic Change 95, 499-521. https://doi.org/10.1007/s10584-009-9583-5.
13. Carter, J., Leeson, A., Orr, A., Kittel, C., & van Wessem, J. M. (2022) Variability in Antarctic surface climatology across regional climate models and reanalysis datasets, The Cryosphere, 16, 3815–3841, https://doi.org/10.5194/tc-16-3815-2022.
14. Cavazos, T., Luna-Niño, R., Cerezo-Mota, R., Fuentes-Franco, R., Méndez, M., Pineda Martínez, L.F., & Valenzuela, E. (2019) Climatic trends and regional climate models intercomparison over the CORDEX-CAM (Central America, Caribbean, and Mexico) domain. International Journal of Climatology, 40(3), 1396–1420. https://doi.org/10.1002/joc.6276.
15. Caya D, Laprise R (1999) A semi-implicit semi-Lagrangian regional climate model: The Canadian RCM. Monthly Weather Review, 127:341–362. https://doi.org/10.1175/1520-0493.
16. Christensen, J.H., Machenhauer, B., Jones R.G., Schär, C., Ruti, P.M., Castro, M., Visconti, G. (1997) Validation of present day regional climate simulations over Europe: LAM simulations with observed boundary conditions. Climate Dynamics, 13, 489–506. https://doi.org/10. 1007/s003820050178.

17. Chotamonsak, C., SalathéJr, E.P., Kreasuwan, J., Chantara, S., Siriwitayakorn, K. (2011) Projected climate change over Southeast Asia simulated using a WRF regional climate model. Atmospheric Science Letters, 12, 213–219. https://doi.org/10.1002/asl.313.
18. Chou, S.C., Nunes, A.M.B. &Cavalcanti, I.F.A. (2000) Extended range forecasts over South America using regional eta model. Journal of Geophysical Research: Atmospheres, 105(D8), 10147–10160. https://doi.org/10.1029/1999JD901137.
19. Choudhary, A., Dimri, A.P. &Maharana, P. (2018) Assessment of CORDEX-SA experiments in representing precipitation climatology of summer monsoon over India. Theoretical and Applied Climatology, 134, 283–307. https://doi.org/10.1007/s00704-017-2274-7.
20. Cook, K.H., Meehl, G.A. &Arblaster, J.M., (2012) Monsoon regimes and processes in CCSM4. Part II: African and American monsoon systems. Journal of Climate, 25(8), 2609-2621.http://dx.doi.org/10.1175/JCLI-D-11-00185.1.
21. Dasari, H.P., Salgado, R., Perdigao, J., Challa, V.S. (2014) A Regional Climate Simulation Study Using WRF-ARW Model over Europe and Evaluation for Extreme Temperature Weather Events.International Journal of Atmospheric Sciences, 704079. https://doi.org/10.1155/2014/704079.
22. Dash, S.K., Mishra, S.K., Sahany, S., Venugopal, V., Karumuri, A. & Gupta, A. (2017) Climate Modeling in India: Present Status and the Way Forward.Bulletin of the American Meteorological Society 98, ES183–ES188.https://doi.org/10.1175/BAMS-D-16-0322.1.
23. Demissie, T.A., Sime, C.H., (2021) Assessment of the performance of CORDEX regional climate models in simulating rainfall and air temperature over southwest Ethiopia. Heliyon 7 (8), e07791. https://doi.org/10.1016/j.heliyon. 2021.e07791.
24. Dickinson, R.E., Errico R.M., Giorgi, F., Bates, G.T. (1989) A regional climate model for the western United States. Climatic Change 15, 383-422. https://doi.org/10.1007/BF00240465.
25. Evans, J.P., Di Virgilio, G., Hirsch, A.L., Hoffmann, P., Remedio, A.R., Ji, F., Rockel, B., Coppala, E. (2021) The CORDEX-Australasia ensemble: evaluation and future projections. Climate Dynamics 57, 1385–1401. https://doi.org/10.1007/s00382-020-05459-0.
26. Falco, M., Carril, A.F., Menéndez, C.G., Zaninelli, P.G., Laurent, Z.X.Li. (2019) Assessment of CORDEX simulations over South America: added value on seasonal climatology and resolution considerations. Climate Dynamics 52, 4771-4786. https://doi.org/10.1007/s00382-018-4412-z.
27. Fasullo, J., Webster, P.J. (2003) A hydrological definition of Indian monsoon onset and withdrawal. Journal of Climate 16(19), 3200-3211.https://doi.org/10.1175/1520-0442.
28. Fonseca, R., & Martín-Torres, J. (2019) High-resolution dynamical downscaling of re-analysis data over the Kerguelen Islands using the WRF model. Theoretical and Applied Climatology 135, 1259-1277. https://doi.org/10.1007/s00704-018-2438-0.
29. Gao, Y., Wang, H.J., Jiang, D.B. (2015) An intercomparison of CMIP5 and CMIP3 models for interannual variability of summer precipitation in Pan-Asian monsoon region. International Journal of Climatology 35:3770–3780. https://doi.org/10.1002/joc.4245.

30. Gao, Y., Xiao, L., Chen, D., Chen, F., Xu, J., Xu,Y.(2017) Quantification of the relative role of land-surface processes and large-scale forcing in dynamic downscaling over the Tibetan Plateau. Climate Dynamics 48, 1705–1721. https://doi.org/10.1007/s00382-016-3168-6.
31. Gent, P.R., Danabasoglu, G., Donner, L.J., Holland M.M., Elizabeth, C.H., Jayne, S.R., Lawrence, D.M., Neale, R.B., Rasch, P.J., Vertenstein, M., Worley, P.H., Yang, ZL. & Zhang, M. (2011) The Community Climate System Model Version 4. Journal of Climate 24(19):4973–4991. https://doi.org/10.1175/2011JCLI4083.1.
32. Ghosh, S., Vittal, H., Sharma, T., Karmakar, S., Kasiviswanathan, K. S., Dhanesh, Y., Sudheer, K.P., Gunthe, S.S. (2016) Indian summer monsoon rainfall: implications of contrasting trends in the spatial variability of means and extremes. PLOS ONE 11 (7), e0158670.https://doi.org/10.1371/journal.pone.0158670.
33. Giorgi, F., & Bates, G.T. (1989) The climatological skill of a Regional Model over complex terrain. Monthly Weather Review 117, 2325-2347.https://doi.org/10.1175/1520-0493.
34. Giorgi, F. (1990) Simulation of Regional Climate using a Limited Area Model nested in a General Circulation Model. Journal of Climate 3, 941–963. https://doi.org/10.1175/1520-0442.
35. Giorgi, F. (2019) Thirty years of Regional Climate Modeling: Where are we and where are we going next? Journal of Geophysical Research: Atmospheres 124, 5696-5723. https://doi.org/10.1029/2018JD030094.
36. Glisan, J. M. &GutowskiJr, W. J. (2014) WRF summer extreme daily precipitation over the CORDEX Arctic, Journal of Geophysical Research: Atmospheres, 119. https://doi.org/10.1002/2013JD020697.
37. Gomes, H.B., Lemos da Silva, M.C., Barbosa, H.d.M.J., Ambrizzi, T., Baltaci, H., Gomes, H.B., Silva, F.D.d.S., Costa, R.L., Figueroa, S.N., Herdies, D.L., PauliquevisJúnior, T.M. (2022) WRF Sensitivity for Seasonal Climate Simulations of Precipitation Fields on the CORDEX South America Domain. Atmosphere 13, 107. https://doi.org/10.3390/atmos13010107.
38. Gu, H., Yu, Z., Yang, C., Ju, Q., Yang, T., and Zhang, D. (2018) High-resolution ensemble projections and uncertainty assessment of regional climate change over China in CORDEX East Asia. Hydrology and Earth System Science, 22, 3087-3103. https://doi.org/10.5194/hess-22-3087-2018.
39. Guhathakurta, P. & Rajeevan, M. (2008) Trends in the rainfall pattern over India. International Journal of Climatology 28(11) 1453-1469. https://doi.org/10.1002/joc.1640.
40. Halder, S., Saha, S. K., Dirmeyer, P. A., Chase, T. N., and Goswami, B. N. (2016) Investigating the impact of land-use land-cover change on Indian summer monsoon daily rainfall and temperature during 1951–2005 using a regional climate model. Hydrology and Earth System Sciences 20, 1765–1784, https://doi.org/10.5194/hess-20-1765-2016.
41. Heikkila, U., Sandvik, A. & Sorteberg, A. (2011) Dynamical downscaling of ERA-40 in complex terrain using the WRF regional climate model. Climate Dynamics 37,1551–1564. https://doi.org/10.1007/s00382-010-0928-6.
42. Hernández-Díaz, L., Laprise, R., Sushama, L., Martynov, A., Winger, K. &Dugas, B. (2013) Climate simulation over CORDEX Africa domain using the fifth-generation Canadian Regional Climate Model

(CRCM5). Climate Dynamics 40, 1415-1433. https://doi.org/10.1007/s00382-012-1387-z.

43. Hirakuchi, H., Giorgi, F. (1995) Multiyear present day and 2XCO2 simulations of monsoon-dominated climate over Eastern Asia and Japan with a regional climate model nested in a general circulation model. Journal of Geophysical Research 100, 21105-21126. https://doi.org/10.1029/95JD01885.
44. Hong, S.Y., Noh, Y., & Dudhia, J. (2006) A new vertical diffusion package with an explicit treatment of entrainment processes. Monthly Weather Review 134(9), 2318- 2341. https://doi.org/10.1175/mwr3199.1.
45. Huo, Y., &Peltier, W.R. (2020) Dynamically downscaled climate change projections for the South Asian Monsoon: mean and extreme precipitation changes and physics parameterization impacts. Journal of Climate, 33(6), 2311-2331.https://doi.org/10.1175/JCLI-D-19-0268.1.
46. Iacono, M.J., Delamere, J.S., Mlawer, E.J., Shephard, M.W., Clough, S.A., Collins, W.D. (2008) Radiative forcing by long-lived greenhouse gases: Calculations with the AER radiative transfer models. Journal of Geophysical Research: Atmospheres 113, D13103. https://doi.org/10.1029/2008JD009944.
47. Iqbal, W., Syed, F.S., Sajjad, H., Nikulin, G., Kjellstrom, E. &Hannachi, A. (2017) Mean climate and representation of jet streams in the CORDEX South Asia simulations by the regional climate model RCA4. Theoretical and Applied Climatology 129, 1-19. https://doi.org/10.1007/s00704-016-1755-4.
48. Islam, S.u., Tang, Y. & Jackson, P.L. (2013) Asian monsoon simulations by Community Climate Models CAM4 and CCSM4. Climate Dynamics 41, 2617-2642. https://doi.org/10.1007/s00382-013-1752-6.
49. Jacob, D., Teichmann, C., Sobolowski, S. et al.(2020). Regional climate downscaling over Europe: perspectives from the EURO-CORDEX community. Regional Environmental Change 20, 51.https://doi.org/10.1007/s10113-020-01606-9.
50. Janjic ZI (2000) Comments on development and evaluation of a convection scheme for use in climate models. Journal of the Atmospheric Sciences 57, 3686. https://doi.org/10.1175/1520-0469.
51. Jones, R.G., Murphy, J.M., Noguer, M. (1995) Simulations of climate change over Europe using a nested regional climate model. I: Assessment of control climate, including sensitivity to location of lateral boundaries. Quarterly Journal of Royal Meteorological Society 121, 1413-1449.https://doi.org/10.1002/qj.49712152610.
52. Jones, R.G., Murphy, J.M., Noguer, M., Keen, A.B. (1997) Simulation of climate change over Europe using a nested regional climate model. II: Comparison of driving and regional model responses to a doubling of carbon dioxide. Quarterly Journal of Royal Meteorological Society 123, 265-292. https://doi.org/10.1002/qj.49712353802.
53. Karmacharya, J., Levine, R.C., Jones, R., Moufouma-Okia, W. & New, M. (2015) Sensitivity of systematic biases in South Asian summer monsoon simulations to regional climate model domain size and implications for downscaled regional process studies. Climate Dynamics 45, 213-231. https://doi.org/10.1007/s00382-015-2565-6.
54. Katzenberger, A., Schewe, J., Pongratz, J., &Levermann, A. (2021) Robust increase of Indian monsoon rainfall and its variability under future warming in CMIP6 models. Earth System Dynamics, 12(2),

367–386. https://doi.org/10.5194/esd-12-367-2021.

55. Kida, H., Koide, T., Sasaki, H. & Chiba, M. (1991) A new approach for coupling a limited area model to a GCM for Regional Climate Simulations. Journal of the Meteorological Society of Japan 69, 723-728. https://doi.org/10.2151/jmsj1965.69.6_723.
56. Kim, G., Cha, DH., Park, C., Jin, C.S., Lee, D.K., Suh, M.S., Oh, S.G., Hong, S.Y., Ahn, J.B., Min, S.K. & Kang, H.S. (2021) Evaluation and Projection of Regional Climate over East Asia in CORDEX-East Asia Phase I Experiment. Asia-Pacific Journal of Atmospheric Sciences 57, 119-134. https://doi.org/10.1007/s13143-020-00180-8.
57. Koenigk, T., Berg, P.&Döscher, R. (2015) Arctic climate change in an ensemble of regional CORDEX simulations. Polar Research 34.https://doi.org/10.3402/polar.v34.24603.
58. Kothawale, D.R.& Rajeevan, M. (2017) Monthly, Seasonal and Annual rainfall time series for all-India, Homogeneous regions and meteorological subdivisions: 1871–2016, IITM Research Report no.RR-138
59. Kumar, K. K., Patwardhan, S. K., Kulkarni, A., Kamala, K., Rao, K. K., & Jones, R. (2011) Simulated projections for summer monsoon climate over India by a high-resolution regional climate model (PRECIS). Current Science, 101(3), 312-326. http://www.jstor.org/stable/24078510.
60. Kumar, D., Rai, P. &Dimri, A.P. (2020) Investigating Indian summer monsoon in coupled regional land-atmosphere downscaling experiments using RegCM4. Climate Dynamics 54, 2959-2980.https://doi.org/10.1007/s00382-020-05151-3.
61. Laprise, R., Hernández-Díaz, L., Tete, K., Sushama, L., Šeparović, L., Martynov, A., Winger, K. &Valin, M. (2013) Climate projections over CORDEX Africa domain using the fifth-generation Canadian Regional Climate Model (CRCM5). Climate Dynamics 41, 3219-3246.https://doi.org/10.1007/s00382-012-1651-2.
62. Ma, J., Wang, H., Fan, K. (2015) Dynamic downscaling of summer precipitation prediction over China in 1998 using WRF and CCSM4.Advances in Atmospheric Sciences 32(5), 577–584.https://doi.org/10.1007/s00376-014-4143-y.
63. Machenhauer, B., Windelband, M., Botzet, M., Hesselbjerg-Christensen, J., Déqué, M., Jones, R.G., Ruti, P.M., Visconti, G. (1998) Validation and analysis of regional present-day climate and climate change simulations over Europe. MPI Report No.275, MPI, Hamburg, Germany, 58 pp. https://hdl.handle.net/21.11116/0000-0005-803D-6.
64. Maharana, P., Dimri, A.P. (2014) Study of seasonal climatology and interannual variability over India and its subregions using a regional climate model (RegCM3). Journal of Earth System Science 123, 1147-1169. https://doi.org/10.1007/s12040-014-0447-7.
65. Maity, S., Satyanarayana, A.N.V., Mandal, M., Nayak, S. (2017) Performance evaluation of land surface models and cumulus convection schemes in the simulation of Indian summer monsoon using a regional climate model. Atmospheric Research 197, 21-41. https://doi.org/10.1016/j.atmosres.2017.06.023.

66. Majra, J.P. & Gur, A. (2009) Climate change and health: Why should India be concerned? Indian Journal of Occupational and Environmental Medicine.13(1): 11-16. https://doi.org/10.4103/0019-5278.50717.
67. Martynov, A., Laprise, R., Sushama, L., Winger, K., Šeparović, L., Dugas, B. (2013) Reanalysis-driven climate simulation over CORDEX North America domain using the Canadian Regional Climate Model, version 5: model performance evaluation. ClimateDynamics 41, 2973-3005.https://doi.org/10.1007/s00382-013-1778-9.
68. Mathison, C., Wiltshire, A., Dimiri, A.P., Falloon, P., Jacob, D., Kumar, P., Moors, E., Ridley, J., Siderius, C., Stoffel, M., Yasunari, T. (2012) Regional projections of North Indian climate for adaptation studies, Science of the Total Environment 468-469S, pp. S4-S17. https://doi.org/10.1016/j.scitotenv.2012.04.066.
69. Maurya, R.K., Sinha, S.P., Mohanty, M.R., Mohanty, U.C. (2018) RegCM4 model sensitivity to horizontal resolution and domain size in simulating the Indian summer monsoon. Atmospheric Research 210, pp 15-33. https://doi.org/10.1016/j.atmosres.2018.04.010.
70. Menendez, C.G., Saulo, A. & Li, Z. X. (2001) Simulation of South American wintertime climate with a nesting system. Climate Dynamics 17, 219–231. https://doi.org/10.1007/s00382000017.
71. Meyer, J.D.D., Jin, J. (2016) Bias correction of the CCSM4 for improved regional climate modeling of the North American monsoon. Climate Dynamics 46, 2961-2976.https://doi.org/10.1007/s00382-015-2744-5.
72. Meyer, J.D.D., Jin, J. (2017) The response of future projections of the North American monsoon when combining dynamical downscaling and bias correction of CCSM4 output. Climate Dynamics 49, 433-447. https://doi.org/10.1007/s00382-016-3352-8.
73. Misra, V., Dirmeyer, P.A., Kirtman, B.P., Juang, H.M. & Kanamitsu, M. (2002b) Regional simulation of interannual variability over South America. Journal of Geophysical Research: Atmospheres 107, LBA 3.1–3.16. https://doi.org/10.1029/2001JD900216.
74. Misra, V., Dirmeyer, P.A., Kirtman, B.P. (2003) Dynamic downscaling of seasonal simulations over South America. Journal of Climate, vol. 16, no. 1, pp. 103-117. https://doi.org/10.1175/1520-0442.
75. Moss, R.H., Edmonds, J.A., Hibbard, K.A., Manning, M.R., Rose, S.K., Van Vuuren, D.P., Carter, T.R., Emori, S., Kainuma, M., Kram, T., Meehl, G.A., Mitchell, J.F.B., Nakicenovic, N., Riahi, K., Smith, S.J., Stouffer, R.J., Thomson, A.M., Weyant, J.P., Wilbanks, T.J. (2010) The next generation of scenarios for climate change research and assessment. Nature 463, 747-756. https://doi.org/10.1038/nature08823.
76. Nastos, P.T., Kapsomenakis, J. (2015) Regional climate model simulations of extreme air temperature in Greece. Abnormal or common records in the future climate? Atmospheric Research 152, 43–60. https://doi.org/10.1016/j.atmosres.2014.02.005.
77. Neale, R.B., Richter, J., Park, S., Lauritzen, P.H., Vavrus, S.J., Rasch, P.J., Zhang, M. (2013) The mean climate of the community atmosphere model (CAM4) in forced SST and fully coupled experiments. Journal of Climate 26, 5150-5168.https://doi.org/10.1175/JCLI-D-12-00236.1.

78. Nicolini, M., Salio,P., Katzfey, J.J., McGregor,J.L., Saulo, A.C. (2002) January and July regional climate simulation over South America. Journal of Geophysical Research: Atmospheres 107(D22): ACL 12-1-ACL 12-13. https:doi.org/10.1029/2001JD000736.
79. Nishant, N., Evans, J. P., Di Virgilio, G., Downes, S. M., Ji, F., Cheung, K. K. W., Tam, E., Miller, J., Beyer, K., Riley, M.L. (2021) Introducing NARCliM1.5: Evaluating the performance of regional climate projections for southeast Australia for 1950-2100. Earth's Future, 9, e2020EF001833.https://doi.org/10.1029/2020EF001833.
80. Niu, X., Wang, S., Tang, J., Lee, D.K., Gutowski, W., Dairaku, K., McGregor, J., Katzfey, J., Gao, X., Wu, J., Hong, S., Wang, Y., Sasaki, H (2015) Projection of Indian summer monsoon climate in 2041-2060 by multiregional and global climate models, Journal of Geophysical Research: Atmospheres 120, 1776-1793. https://doi.org/10.1002/2014JD022620.
81. Nobre, P., Moura, A.D. & Sun, L. (2001) Dynamical downscaling of seasonal climate prediction over Nordeste Brazil with ECHAM3 and NCEP's regional spectral models at IRI. Bulletin of the American Meteorological Society, vol. 82, no. 12, pp. 2787-2796. https://doi.org/10.1175/1520-0477.
82. Outten, S. &Sobolowski, S. (2021) Extreme wind projections over Europe from the Euro-CORDEX regional climate models. Weather and Climate Extremes 33, Article 100363.https://doi.org/10.1016/j.wace.2021.100363.
83. Öztürk, T., Altinsoy, H., Türkeş, M. &Kurnaz, M. L. (2012) Simulation of temperature and precipitation climatology for the Central Asia CORDEX domain using RegCM 4.0. Climate Research 52(1), 63-76. http://doi.org/10.3354/cr01082.
84. Pai, D.S., Sridhar, L., Badwaik, M.R., Rajeevan, M. (2014) Analysis of the daily rainfall events over India using a new long period (1901–2010) high resolution (0.25° × 0.25°) gridded rainfall data set. Climate Dynamics 45 (3-4), pp. 755-776. https://doi.org/10. 1007/s00382-014-2307-1.
85. Parthasarathy, B., Munot, A. A. &Kothawale, D.R. (1994) All-India monthly and seasonal rainfall series: 1871-1993. Theoretical and Applied Climatology 49(4) 217-224. https://doi.org/10. 1007/BF00867461.
86. Parthasarathy, B., Munot, A.A. & Kothawale, D.R. (1995) Monthly and seasonal rainfall series for all India homogenous regions and meteorological sub-divisions: 1871-1994. Research Report no.RR-065, Indian Institute of Tropical Meteorology Pune, pp 113.
87. Pattnayak, K.C., Panda, S.K., Saraswat, V. & Dash, S.K. (2018) Assessment of two versions of regional climate model in simulating the Indian Summer Monsoon over South Asia CORDEX domain.Climate Dynamics 50, 3049-3061.https://doi.org/10.1007/s00382-017-3792-9.
88. Polanski, S., Rinke, A., Dethloff, K. (2010) Validation of the HIRHAM-Simulated Indian Summer Monsoon Circulation. Advances in Meteorology, vol. 2010, Article ID 415632, 14 pages, 2010.https://doi.org/10.1155/2010/415632.
89. Plummer, D.A., Caya, D., Frigon, A., Côté, H., Giguère, M., Paquin, D., Biner, S., Harvey, R. & de Elia, R. (2006) Climate and climate change over North America as simulated by the Canadian RCM. Journal of Climate 19, 3112-3132. https://doi.org/10.1175/JCLI3769.1.

90. Prein, A.F., Bukovsky, M.S., Mearns, L.O., Bruyère, C.L. & Done, J.M. (2019) Simulating North American Weather Types With Regional Climate Models. Frontiers in Environmental Science 7:36. https://doi.org/10.3389/fenvs.2019.00036.
91. Qiu, Y., Hu, Q., Zhang, C. (2017) WRF simulation and downscaling of local climate in Central Asia. International Journal of Climatology 37, 513–528. https://doi.org/10.1002/joc.5018.
92. Raghavan, S.V., Vu, M.T., Liong, S.Y. (2016) Regional climate simulations over Vietnam using the WRF model. Theoretical and Applied Climatology 126, 161-182. https://doi.org/10.1007/s00704-015-1557-0.
93. Rai, P., Joshi, M., Dimri, AP., Turner, AG. (2018) The role of potential vorticity anomalies in the Somali Jet on Indian Summer Monsoon Intraseasonal Variability. Climate Dynamics 50(11–12), 4149–4169.https://doi.org/10.1007/s00382-017-3865-9.
94. Rai, P., Ziegler, K., Abel, D., Pollinger, F., Paeth, H (2022) Performance of a regional climate model with interactive vegetation (REMO-iMOVE) over Central Asia. Theoretical and Applied Climatology 150, 1385-1405. https://doi.org/10.1007/s00704-022-04233-y.
95. Raju, P.V.S., Bhatla, R., Almazroui, M., Assiri, M., (2015) Performance of convection schemes on the simulation of summer monsoon features over the South Asia CORDEX domain using RegCM-4.3. International Journal of Climatology 35, 4695-4706.https://doi.org/10.1002/joc.4317.
96. Ramakrishna, S.S.V.S., Brahmananda Rao, V., Srinivasa Rao, B.R., Hari Prasad, D., Nanaji Rao, N., Roshmitha Panda. (2017) A study of 2014 record drought in India with CFSv2 model: role of water vapor transport. Climate Dynamics 49, 297-312. https://doi.org/10.1007/s00382-016-3343-9.
97. Ramakrishna, S.S.V.S., Ravi Srinivasa Rao, B., Satyanarayana, G.C., Nanaji Rao, N., Roshmitha Panda, MadhuSai, S., SaiVenkataRamana, M., Bhaskar Rao, D.V. (2022) Simulation of Regional Climate over the Indian subcontinent through dynamical downscaling using WRF ARW model. Theoretical and Applied Climatology 148, 391- 413. https://doi.org/10.1007/s00704-021-03905-5.
98. Rana, A., Nikulin, G., Kjellström, E., Strandberg, G., Kupiainen, M., Hansson, U. &Kolax, M. (2020) Contrasting regional and global climate simulations over South Asia. Climate Dynamics 54, 2883-2901.https://doi.org/10.1007/s00382-020-05146-0.
99. Ratna, S.B., Ratnam, J.V., Behera, S.K., Tangang, F.T., Yamagata, T. (2017) Validation of the WRF regional climate model over the subregions of Southeast Asia: climatology and interannualvariability.Climate Research 71(3), pp.263-280.https://doi.org/10.3354/cr01445.
100. Rivera, E.R., Amador, J.A. &Sáenz, F. (2022) Sensitivity of precipitation and atmospheric low-level circulation patterns to domain size and choice of parameterization schemes in RegCM4.4 over Central America. Climate Research 89, 61-83. https://doi.org/10.3354/cr01707.
101. Rojas, M. & Seth, A. (2003) Simulation and sensitivity in a nested modeling system for South America-part II: GCM boundary forcing. Journal of Climate, vol. 16, pp. 2454-2471. https://doi.org/10.1175/1520-0442.
102. Russo, E., Kirchner, I., Pfahl, S., Schaap, M., and Cubasch, U. (2019) Sensitivity studies with the regional climate model COSMO-CLM 5.0 over the CORDEX Central Asia Domain. Geoscientific Model

Development 12, 5229-5249.https://doi.org/10.5194/gmd-12-5229-2019.

103. Saeed, F., Hagemann, S. & Jacob, D. (2012) A framework for the evaluation of the South Asian summer monsoon in a regional climate model applied to REMO. International Journal of Climatology 32, 430-440. https://doi.org/10.1002/joc.2285.
104. Schneider, S.H. & Dickinson, R.E. (1974) Climate Modeling. Review of Geophysical Space Physics, 12, 447-493. http://dx.doi.org/10.1029/RG012i003p00447.
105. Seth, A. & Rojas, M. (2003) Simulation and sensitivity in a nested modeling system for South America-part I: reanalysis boundary forcing. Journal of Climate, vol. 16, pp. 2437-2453. https://doi.org/10.1175/1520-0442.
106. Singh, S., Mall, R. K., Dadich, J., Verma, S., Singh, J. V. & Gupta, A. (2021) Evaluation of CORDEX-South Asia regional climate models for heat wave simulations over India. Atmospheric Research vol.248, 105228.https://doi.org/10.1016/j.atmosres.2020.105228.
107. Skamarock, W.C., Klemp, J.B., Dudhia, J., Gill, D.O., Barker, D., Duda, M.G., … Powers, J.G. (2008) A Description of the Advanced Research WRF Version 3 (No.NCAR/TN-475+STR).University Corporation for Atmospheric Research. https://doi.org/10.5065/D68S4MVH.
108. Srivastava, A.K., Rajeevan, M., Kshirsagar, S.R. (2009) Development of a high resolution daily gridded temperature data set (1969-2005) for the Indian region. Atmospheric Science Letters 10, 249-254. https://doi.org/10.1002/asl.232.
109. Souverijns, N., Gossart, A., Demuzere, M., Lenaerts, J. T. M., Medley, B., Gorodetskaya, I. V., Broucke, S.V., Lipzig N.P.M.V. (2019) A new regional climate model for POLAR-CORDEX: Evaluation of a 30-year hindcast with COSMO-CLM2 over Antarctica. Journal of Geophysical Research: Atmospheres 124, 1405-1427. https://doi.org/10.1029/2018JD028862.
110. Stan, C. & Xu, L. (2015) Climate simulations and projections with a super-parameterized climate model. Environmental Modelling Software 60, 134-215. https://doi.org/10.1016/j.envsoft.2014.06.013.
111. Syed, F.S., Iqbal, W., Syed, A.A.B. & Rasul, G. (2014) Uncertainties in the regional climate models simulations of South-Asian summer monsoon and climate change. Climate Dynamics 42, 2079-2097. https://doi.org/10.1007/s00382-013-1963-x.
112. Takhsha, M., Nikiéma, O., Lucas-Picher, P., Laprise, R., Hernandez-Diaz, L., Winger, K. (2018) Dynamical downscaling with the fifth-generation Canadian regional climate model (CRCM5) over the CORDEX Arctic domain: effect of large-scale spectral nudging and of empirical correction of sea-surface temperature. Climate Dynamics 51, 161-186. https://doi.org/10.1007/s00382-017-3912-6.
113. Tangang, F., Santisirisomboon, J., Juneng, L., Salimun, E., Chung, J., Supari, S., Cruz, F., Ngai, S.T., Ngo-Duc, T., Singhruck, P., Narisma, G., Santisirisomboon, J., Wongsaree, W., Promjirapawat, K., Sukamongkol, Y., Srisawadwong, R., Setsirichok, D., Phan-Van, T., Aldrian, E., Gunawan, D., Nikulin, G., Yang, H. (2019) Projected future changes in mean precipitation over Thailand based on multi-model regional climate simulations of CORDEX Southeast Asia. International Journal of Climatology 39, 5413-5436.https://doi.org/10.1002/joc.6163.

114. Tangang, F., Chung, J.X., Juneng, L., Supari, Salimun, E., Ngai, S.T., Jamaluddin, A.F., Faisal Mohd, M.S., Cruz, F., Narisma, G., Santisirisomboon, J., Ngo-Duc, T., Tan, P.V., Singhruck, P., Gunawan, D., Aldrian, E., Sopaheluwakan, A., Grigory, N., Remedio, A.R.C., Sein, D.V., Griggs, D.H., McGregor, J.L., Yang, H., Sasaki, H. & Kumar, P. (2020) Projected future changes in rainfall in Southeast Asia based on CORDEX-SEA multi-model simulations. Climate Dynamics 55, pp. 1247-1267, https://doi.org/10.1007/s00382-020-05322-2.
115. Taylor, K.E., Stouffer, R.J. &Meehl, G.A. (2012) An overview of CMIP5 and the experiment design. Bulletin of the American Meteorological Society 93,485-498. https://doi.org/10.1175/BAMS-D-11-00094.1.
116. Turp, M.T., An, N., Collu, K. &Kurnaz, M.L. (2022) Prospective Changes in Climatology of the CORDEX Domain of Australasia: A Dynamical Downscaling Approach Using RegCM4.6. EGU General Assembly 2022, Vienna, Austria, 23-27 May 2022, EGU22-10104. https://doi.org/10.5194/egusphere-egu22-10104.
117. Tyagi, N., Jayal, T., Singh, M., Mandwal, V., Saini, A., Nirbhav, Sahu, N., Nayak, S. (2022) Evaluation of Observed and Future Climate Change Projection for Uttarakhand, India, Using CORDEX-SA. Atmosphere 13, 947. https://doi.org/10.3390/atmos13060947.
118. Vautard, R., Kadygrov, N., Iles, C., Boberg, F., Buonomo, E., Bülow, K., Coppola, E., Corre, L., Meijgaard, E.V., Nogherotto, R., Sandstad, M., Schwingshackl, C., Somot, S., Aalbers, E., Christensen, O.B., Ciarlo, J.M., Demory, M.E., Giorgi, F., Jacob, D., Jones, R.G., Keuler, K., Kjellström, E., Lenderink, G., Levavasseur, G., Nikulin, G., Sillmann, J., Solidoro, C., Sørland, S.L., Steger, C., Teichmann, C., Warrach-Sagi, W., Wulfmeyer, V. (2021) Evaluation of the large EURO-CORDEX regional climate model ensemble. Journal of Geophysical Research: Atmospheres, 126. https://doi.org/10.1029/2019JD032344.
119. Wamahiu, K., Kala, J. &Andrys, J. (2020) Influence of bias-correcting global climate models for regional climate simulations over the CORDEX-Australasia domain using WRF. Theoretical and Applied Climatology 142, 1493-1513. https://doi.org/10.1007/s00704-020-03254-9.
120. Warscher, M., Wagner, S., Marke, T., Laux, P., Smiatek, G., Strasser, U., Kunstmann, H. (2019) A 5 km Resolution Regional Climate Simulation for Central Europe: Performance in High Mountain Areas and Seasonal, Regional and Elevation-Dependent Variations. Atmosphere 10, 682. https://doi.org/10.3390/atmos10110682.
121. Zou, L., Zhou, T. &Peng, D. (2016) Dynamical downscaling of historical climate over CORDEX East Asia domain: A comparison of regional ocean-atmosphere coupled model to stand-alone RCM simulations, Journal of Geophysical Research: Atmospheres 121, 1442-1458. https://doi.org/10.1002/2015JD023912.

Tables

Table: 1 Model Configuration

Dynamics	Details
Model Version	WRF-ARW V3.9
Type	Non-hydrostatic
Domain	15.5^0 E - 116.5^0 E; -16.5^0 S- 47.5^0 N
Resolution	25 km Horizontal resolution (389x274 grid points along E-W x N-S) and 40 Vertical levels
Input data for forcing	CMIP5-CCSM4 RCP6.0
Microphysics	WRF Single-Moment 6-class (WSM-6) (Hong and Lim,2006)
Planetary Boundary layer	Yonsei University Scheme (YSU) (Hong et al. 2006)
Cumulus Physics	Betts–Miller–Janjic (BMJ) (Betts and Miller 1986),(Janjic 2000)
Long wave Radiation	Rapid Radiative Transfer Model for GCMs (RRTMG) (lacono et al.2008)
Short wave Radiation	Rapid Radiative Transfer Model for GCMs (RRTMG)

Table.2. Statistical metrics of regional-scale evaluation of rainfall (mm) of the monsoon season; Mean, Standard deviation, (Root-Mean-Square Error (RMSE) and Correlation Coefficient (CC) are between WRF and IMD rainfall)

Regions	Mean		Standard Deviation		RMSE	Correlation
	IMD	WRF	IMD	WRF		
South Peninsular	28.50	29.90	6.80	5.14	1.403	0.922
West Central	70.83	73.54	21.38	20.69	2.714	0.910
North West	24.49	15.57	9.68	5.92	8.920	0.904
Central North East	37.32	35.73	9.93	10.52	1.593	0.965
North East	31.13	30.92	5.27	7.40	0.210	0.819
All India	217.67	214.39	59.89	58.26	3.284	0.637

Table 3: Statistical metrics of seasonal temperatures of sub-divisions for Pre-monsoon Season

S.No.	Name of the subdivision	Mean (^{0}C)			Standard Deviation (^{0}C)		
		IMD	WRF	CCSM4	IMD	WRF	CCSM4
1.	Assam&Meghalaya	24.22	26.93	22.36	1.65	3.1	2.54
2.	NMMT	24.32	23.67	24.76	1.58	2.72	2.12
3.	Sikkim&West Bengal	25.59	21.94	18.51	1.93	3.55	3.1
4.	Gangetic West Bengal	29.37	30.67	29.53	1.98	2.65	2.77
5.	Odisha	30.14	30.71	30.72	2.05	2.43	2.29
6.	Jharkhand	29.09	30.49	29.44	2.64	3.47	3.39
7.	Bihar	28.08	30.86	28.61	2.75	4.18	3.49
8.	East UttarPradesh	28.75	31.0	29.37	3.5	4.77	3.99
9.	West UttarPradesh	28.01	30.1	29.11	3.89	5.09	4.25
10.	Haryana & CHD &Delhi	27.24	28.96	27.8	4.22	5.61	4.4
11.	Punjab	25.45	28.02	25.77	4.39	5.9	4.5
12.	West Rajasthan	29.6	29.83	31.22	3.73	4.51	4.02
13.	East Rajasthan	29.68	29.93	30.47	3.76	4.36	3.75
14.	West Madhya Pradesh	30.16	30.89	31.16	3.47	3.68	3.44
15.	East Madhya Pradesh	29.8	30.84	30.62	3.58	3.86	3.73
16.	Gujarat	30.37	30.77	31.08	2.48	2.7	2.62
17.	Saurashtra&Kachh	29.73	29.87	30.43	2.15	2.33	2.34
18.	Konkan&Goa	29.03	28.34	28.54	1.5	1.07	1.18
19.	MadhyaMaharashtra	29.75	29.4	30.18	1.81	1.84	1.77
20.	Marathwada	31.13	31.28	31.36	2.32	2.4	2.27
21.	Vidarbha	31.51	32.61	32.21	2.86	2.94	2.87
22.	Chhattisgarh	30.18	30.88	31.22	2.83	3.12	2.92
23.	Coastal Andhra Pradesh	30.93	30.31	30.33	1.79	2.17	1.75
24.	Telangana	31.65	32.02	32.22	2.12	2.39	2.11
25.	Rayalaseema	30.74	30.74	31.06	1.48	1.84	1.76
26.	TamilNadu&Puducherry	29.69	29.15	29.55	1.15	1.58	1.26
27.	Coastal Karnataka	27.67	27.25	28.13	0.76	0.75	0.7

28.	North Interior Karnataka	30.25	30.26	31.22	1.39	1.53	1.55
29.	South Interior Karnataka	27.6	27.16	29.38	0.91	1.07	1.24
30.	Kerala	27.44	26.89	28.55	0.75	0.67	0.73

Table 4: Statistical metrics of seasonal temperatures of sub-divisions for Monsoon Season

S.No	Name of the sub division	Mean(^{0}C)			Standard Deviation (^{0}C)		
		IMD	WRF	CCSM4	IMD	WRF	CCSM4
1.	Assam & Meghalaya	28.57	28.59	25.43	0.6	1.02	0.6
2.	NMMT	27.63	24.93	26.6	0.48	0.87	0.53
3.	Sikkim & West Bengal	28.03	24.78	21.8	0.53	1.33	0.86
4.	Gangetic West Bengal	29.63	30.1	28.952	0.8	1.92	1.11
5.	Odisha	28.53	28.91	28.01	1.21	2.38	1.53
6.	Jharkhand	28.98	30	28.27	1.23	2.81	1.74
7.	Bihar	29.69	32.22	28.5	0.99	2.7	1.83
8.	East Uttar Pradesh	30.08	33.47	29.33	1.54	3.45	2.33
9.	West Uttar Pradesh	29.84	33.87	29.67	1.7	3.37	2.36
10.	Haryana & CHD & Delhi	30.42	34.94	30.23	1.56	3.01	2.1
11.	Punjab	29.74	35.53	29.6	1.44	2.94	2.01
12.	West Rajasthan	30.83	34.07	32.27	1.82	1.63	2.13
13.	East Rajasthan	29.92	31.99	29.77	2.04	2.57	2.38
14.	West Madhya Pradesh	28.49	29.97	28.37	2.12	2.76	2.25
15.	East Madhya Pradesh	28.67	30.11	28.26	2.06	3.36	2.43
16.	Gujarat	28.93	30.16	28.99	1.64	1.56	1.7
17.	Saurashtra&Kachh	29.52	29.92	29.76	1.4	1.2	1.38
18.	Konkan& Goa	26.78	26.57	26.16	0.97	0.95	0.88
19.	MadhyaMaharashtra	26.61	26.07	26.14	1.23	1.29	1.14
20.	Marathwada	27.38	27.33	26.92	1.57	1.96	1.32
21.	Vidarbha	27.97	29.14	27.78	1.9	2.85	2
22.	Chhattisgarh	28.24	29.02	27.72	1.68	3	2
23.	Coastal Andhra Pradesh	29.33	29.32	29.09	1.19	1.87	1.16
24.	Telangana	28.26	28.58	28.3	1.5	2.37	1.41
25.	Rayalaseema	28.21	27.81	28.11	0.98	1.23	0.77
26.	TamilNadu&Puducherry	28.57	27.45	28.31	0.67	0.91	0.53
27.	Coastal Karnataka	24.6	24.78	24.95	0.57	0.66	0.62

28.	North Interior Karnataka	26.55	26.14	26.2	0.98	1.24	0.88
29.	South Interior Karnataka	24.64	23.73	25.42	0.62	0.76	0.63
30.	Kerala	25.42	24.46	26.04	0.5	0.52	0.44

Table 5: Statistical metrics of rainfall of sub-divisions for Monsoon Season

S.No.	Name of the subdivision	Mean (mm/day)			Standard Deviation (mm/day)		
		IMD	WRF	CCSM4	IMD	WRF	CCSM4
1.	Assam&Meghalaya	13.48	12.46	11.05	1.55	1.63	1.64
2.	NMMT	10.22	17.21	6.99	1.08	1.65	0.7
3.	Sikkim&West Bengal	17.51	11.05	16.87	1.77	1.41	2.36
4.	Gangetic West Bengal	8.9	7.68	8.15	1.07	0.99	0.69
5.	Odisha	9.62	9.65	9.63	1.15	1.28	0.9
6.	Jharkhand	8.14	9.16	7.45	1.01	1.27	0.72
7.	Bihar	8.04	7.14	7.06	1.15	1.08	0.78
8.	East UttarPradesh	6.49	6.33	6.1	1.04	1.13	0.75
9.	West UttarPradesh	5.37	5.15	6.07	0.96	1.02	0.73
10.	Haryana & CHD &Delhi	3.71	3.12	5.12	0.67	0.81	0.64
11.	Punjab	4.25	2.12	5.47	0.77	0.49	0.71
12.	West Rajasthan	2.61	1.64	3.84	0.56	0.55	0.68
13.	East Rajasthan	5.61	5.16	5.68	1.04	1.3	0.86
14.	West Madhya Pradesh	7.72	7.69	7.93	1.24	1.66	1.16
15.	East Madhya Pradesh	8	9.58	8.22	1.21	1.67	1.16
16.	Gujarat	7.6	4.72	8.04	1.48	1.41	1.31
17.	Saurashtra&Kachh	5.8	2.1	5.93	1.41	0.73	1.04
18.	Konkan&Goa	25.78	12.84	14.82	3.56	2.41	1.96
19.	MadhyaMaharashtra	5.84	5.92	11.33	0.94	1.38	1.52
20.	Marathwada	5.53	7.43	8.83	0.75	1.57	1.06
21.	Vidarbha	8.2	9.19	9.82	1.06	1.7	1.23
22.	Chhattisgarh	9.36	11.14	9.86	1.08	1.67	1.19
23.	Coastal Andhra Pradesh	5.47	7.56	8.63	0.66	1.14	0.75
24.	Telangana	6.88	8.33	8.81	0.92	1.41	0.87
25.	Rayalaseema	3.74	4.25	6.25	0.6	0.66	0.51
26.	TamilNadu&Puducherry	3.33	3.9	7.07	0.65	0.47	0.56
27.	Coastal Karnataka	22.98	15.27	15.08	2.93	1.93	1.59

28.	North Interior Karnataka	4.29	5.5	9.2	0.64	0.97	0.88
29.	South Interior Karnataka	5.64	6.66	9.72	0.92	0.8	0.87
30.	Kerala	14.79	13.54	11.82	1.9	1.46	1.04

Figures

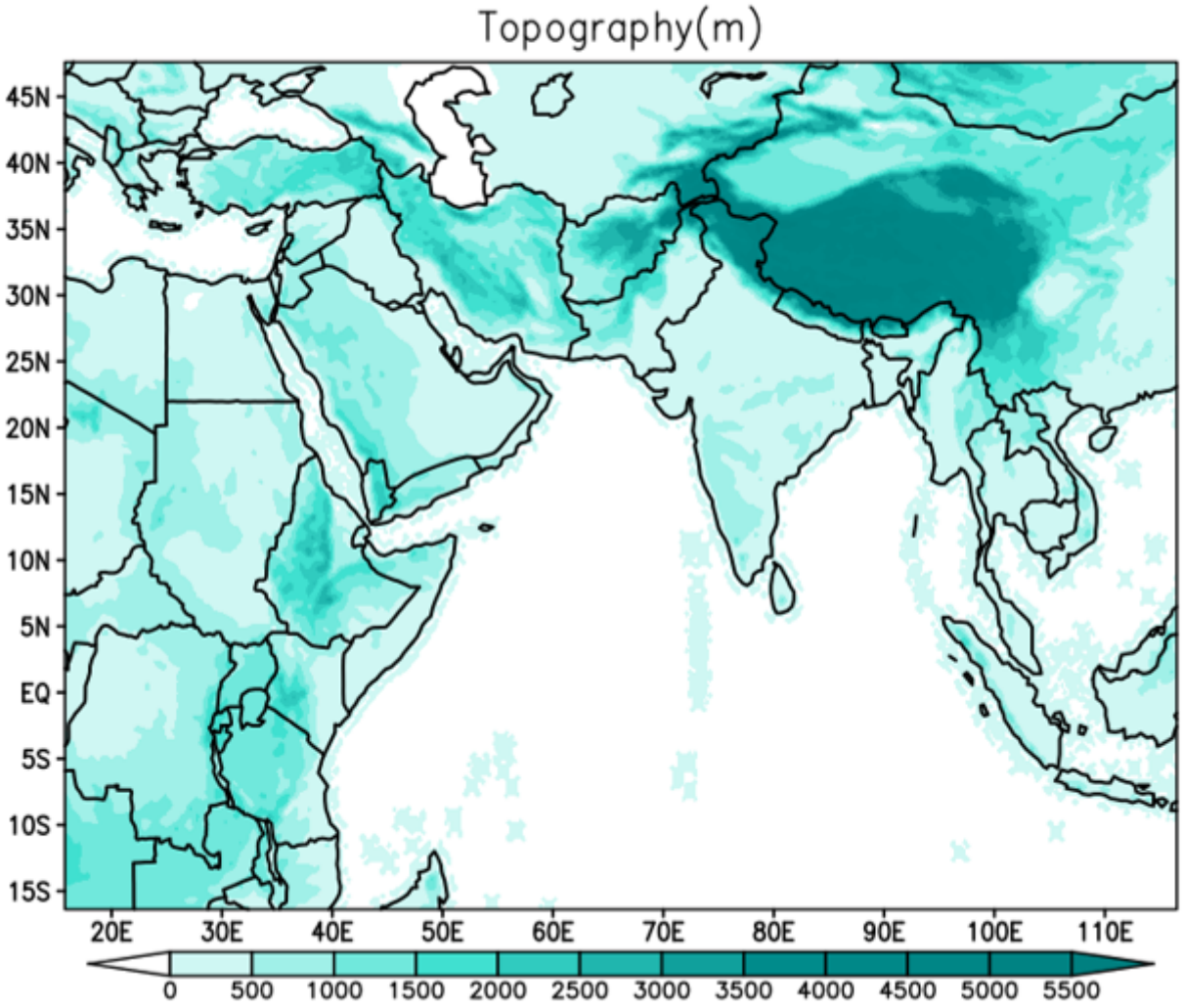

Figure 1

Domain for the study area (South Asia-CORDEX)

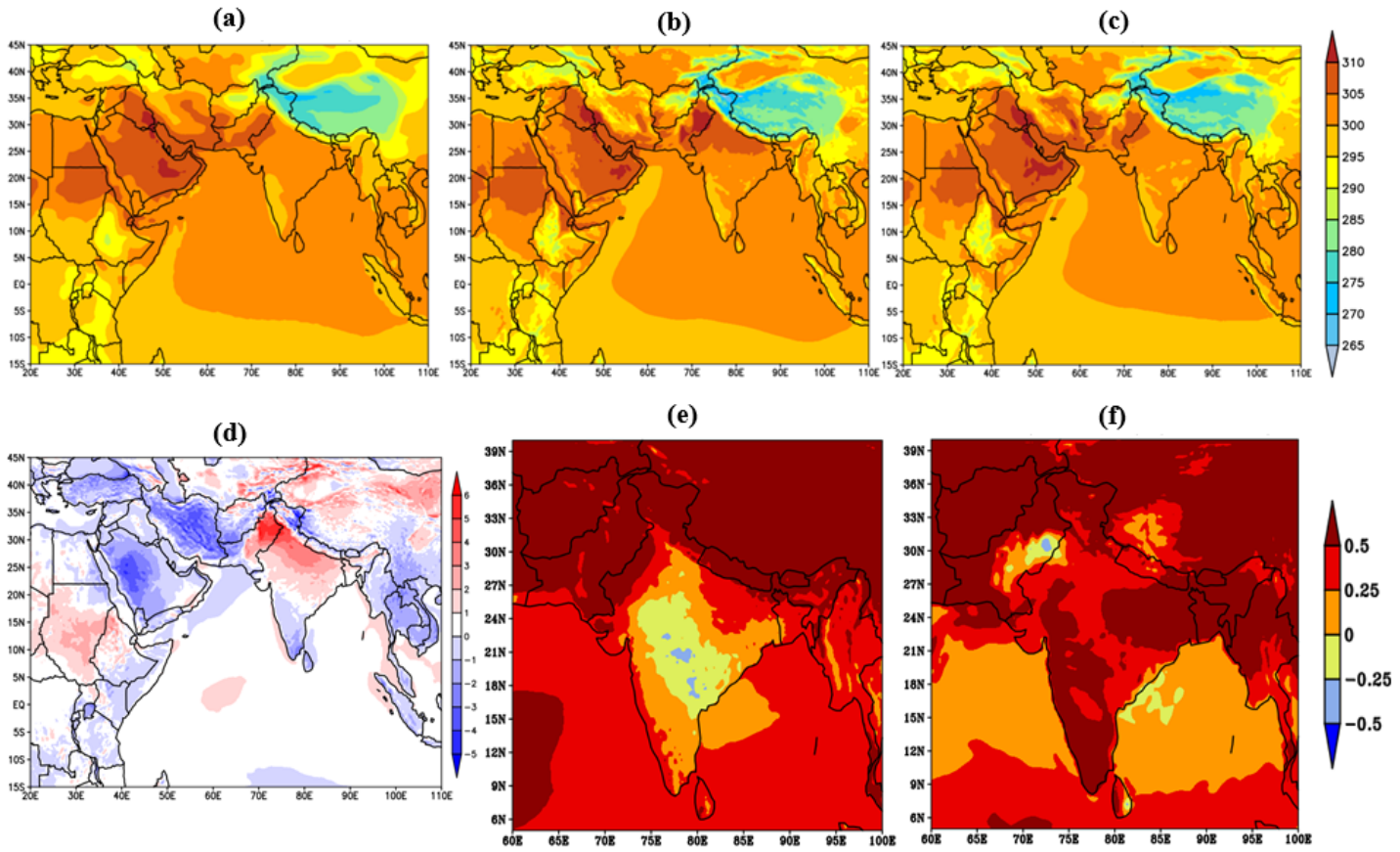

Figure 2

Spatial distribution of the mean near surface air temperature-2m (K) for summer monsoon season for the period 2007-2021 (a-c), (a) CCSM, (b) WRF, (c) ERA5; (d)Bias(WRF-ERA5), Difference of the mean surface temperature for the periods ((2007-2021) minus (1976-2005)) (e)

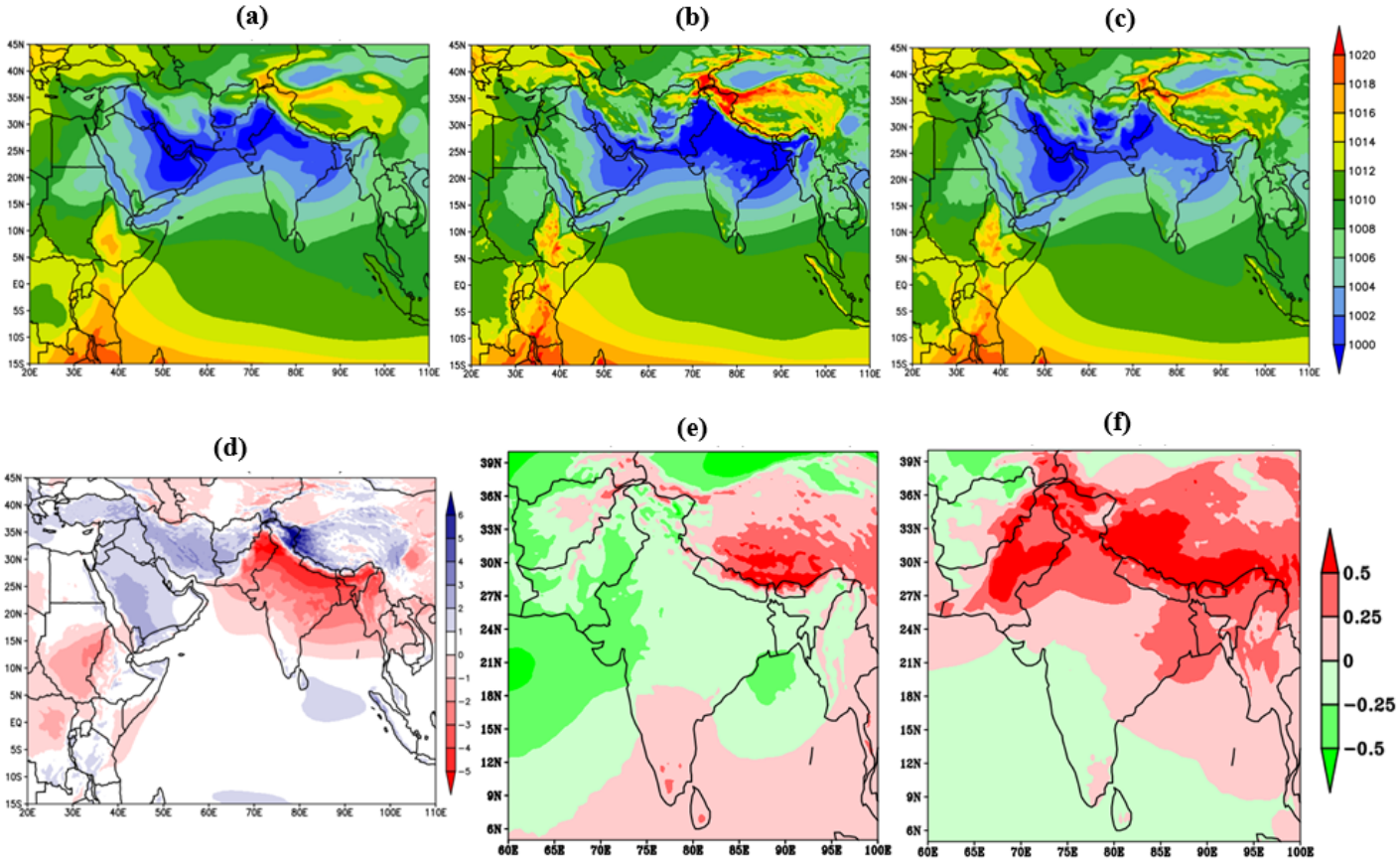

Figure 3

Same as fig.2 but for Mean Sea Level Pressure (MSLP)

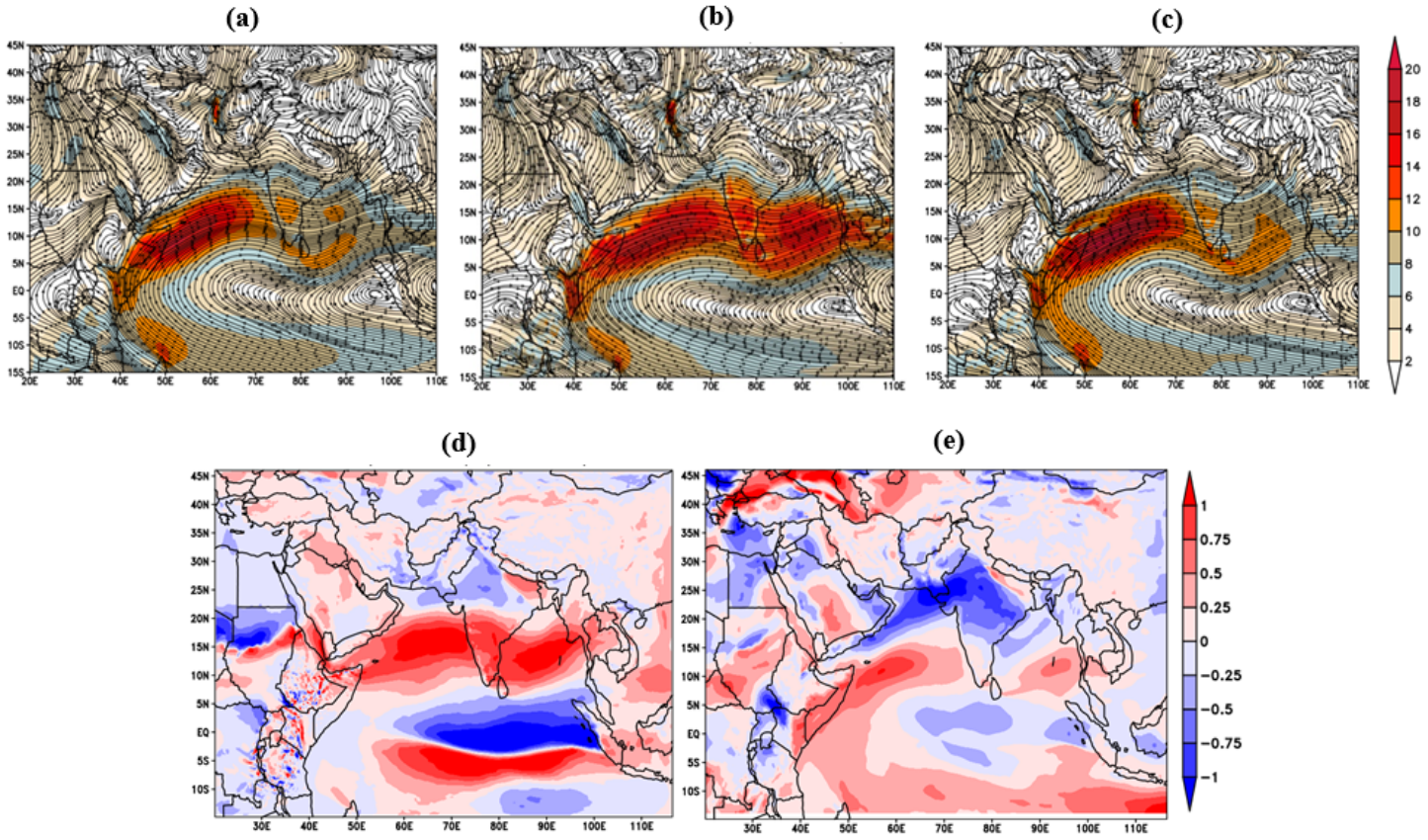

Figure 4

Spatial distribution of mean values of winds at 850 hPa with streamlines and magnitude (shaded) (m/s) for summer monsoon season for the period 2007-2021 (a-c), (a) CCSM, (b) WRF, (c) ERA5; Difference of the winds for the periods ((2007-2021) minus (1976-2005)) (d) WRF (e) ERA5.

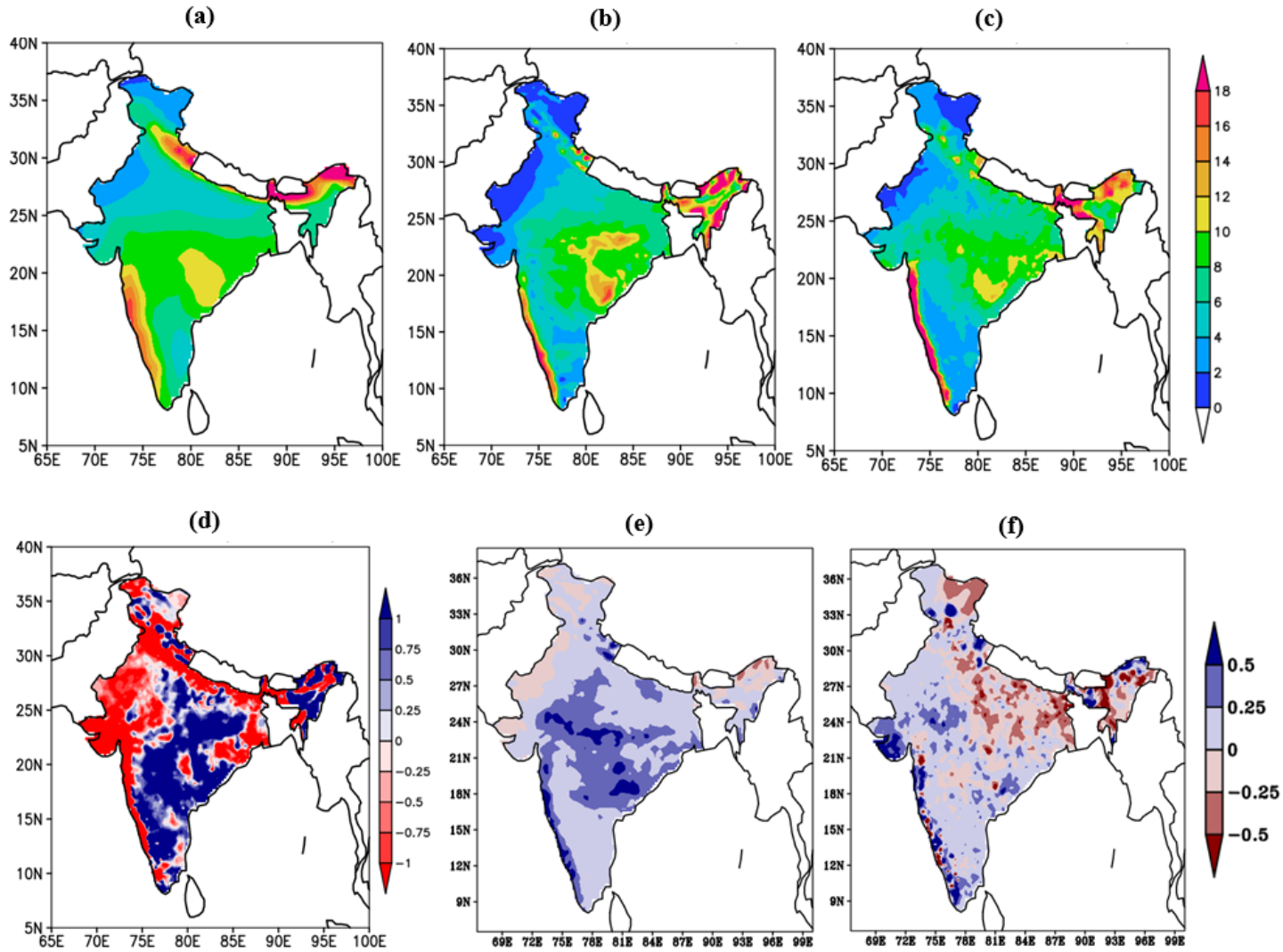

Figure 5

Spatial distribution of mean values of Accumulated rainfall (mm/day) for summer monsoon season for the period 2007-2021 (a-c), (a) CCSM, (b) WRF, (c) IMD; (d) Bias(WRF-IMD), Difference of the mean rainfall for the periods ((2007-2021) minus (1976-2005)) (e) WRF (f) IMD.

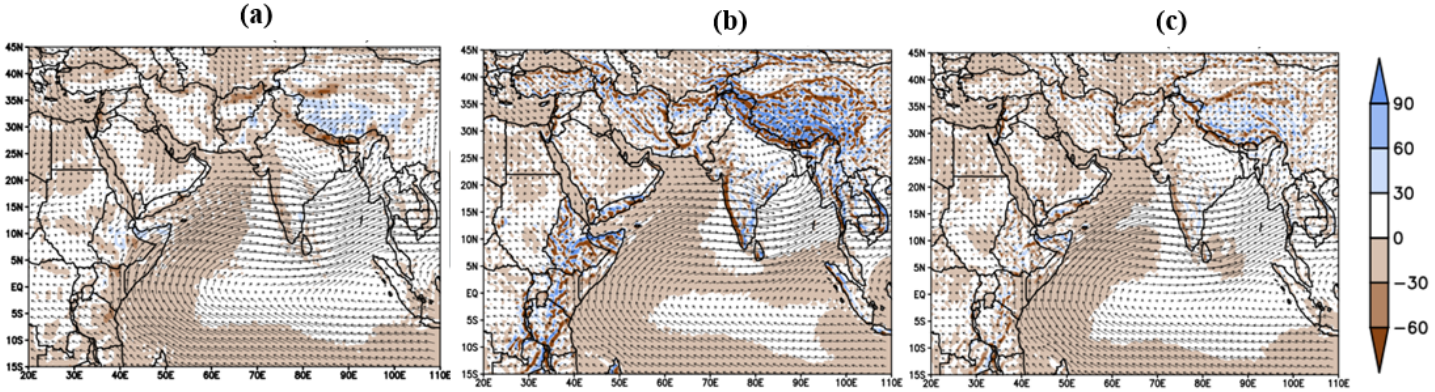

Figure 6

Vertically Integrated Moisture Flux Convergence (VIMFC) for summer monsoon season for the period 2007-2021 (a-c). (a) CCSM, (b) WRF, (c) ERA.

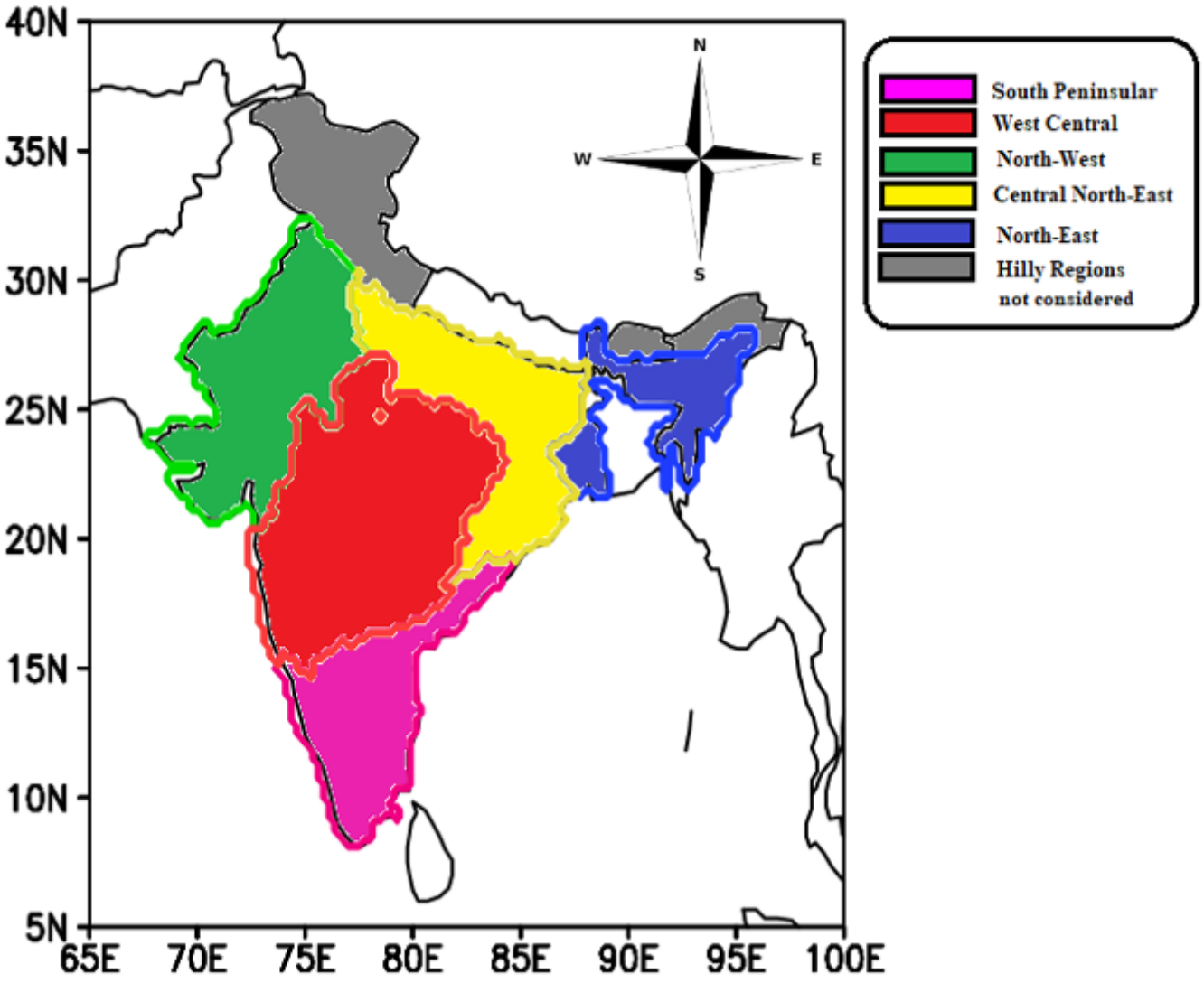

Figure 7

Rainfall Homogenous regions of India

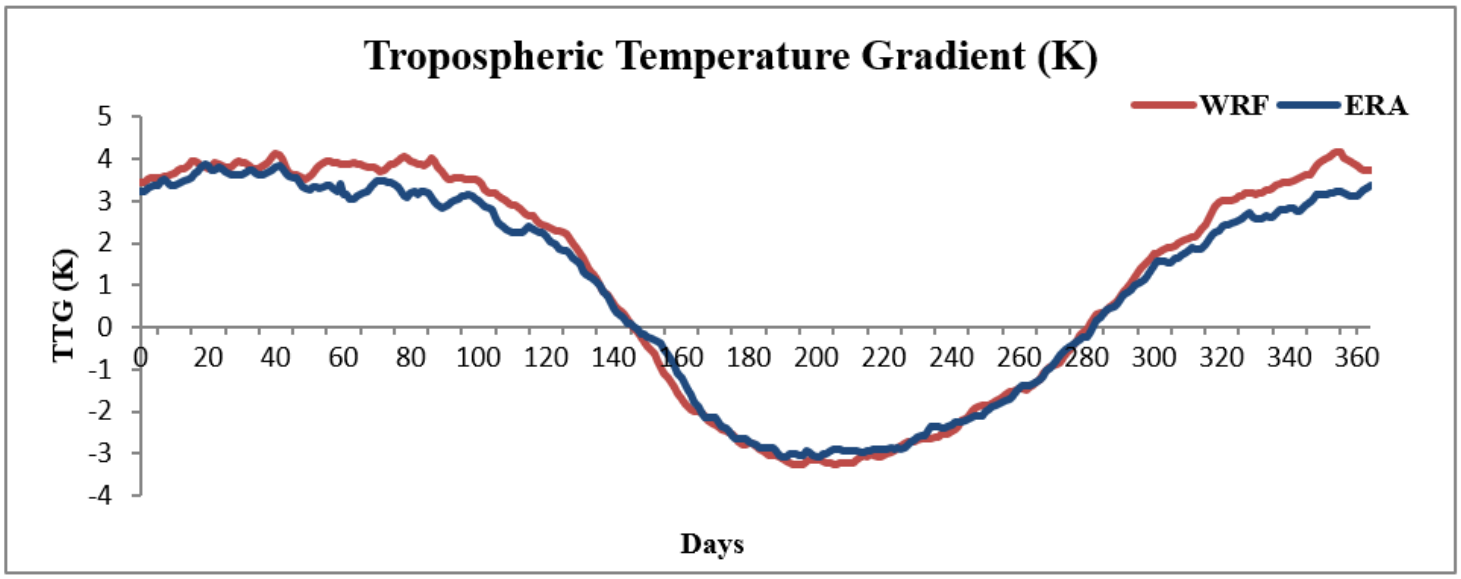

Figure 8

Tropospheric temperature (600–200 hPa) gradient between the southern (15° S–5° N, 40°–100° E) and northern (5°–35° N, 40°–100° E) region from ERA5 reanalysis (Blue) and WRF model (Red) for the period 2007-2021.

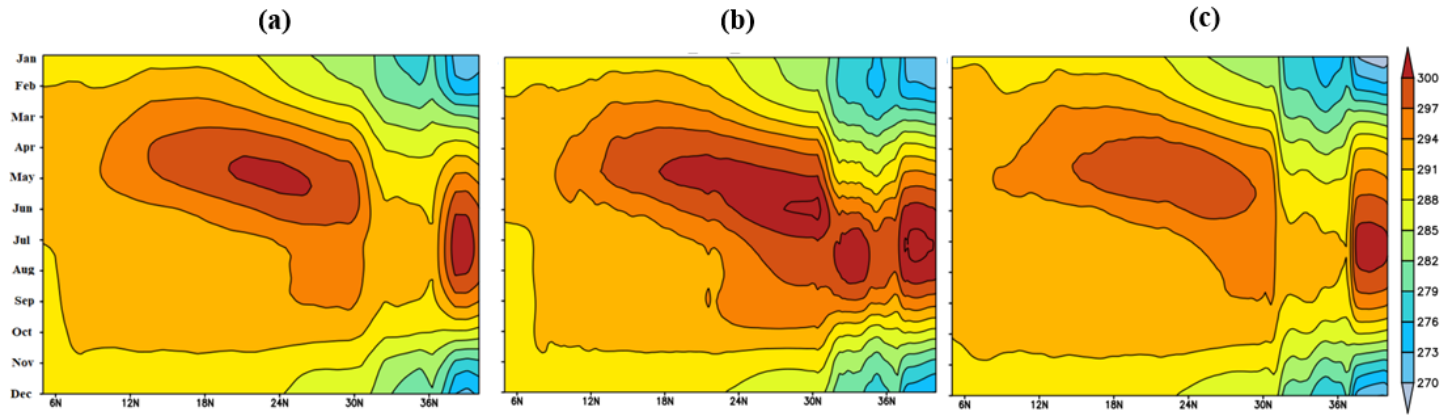

Figure 9

Latitude-time cross section of temperatures (K) at 850 hPa along 78^0E longitude for the summer monsoon season for the period 2007-2021(a) CCSM, (b) WRF, (c) ERA.

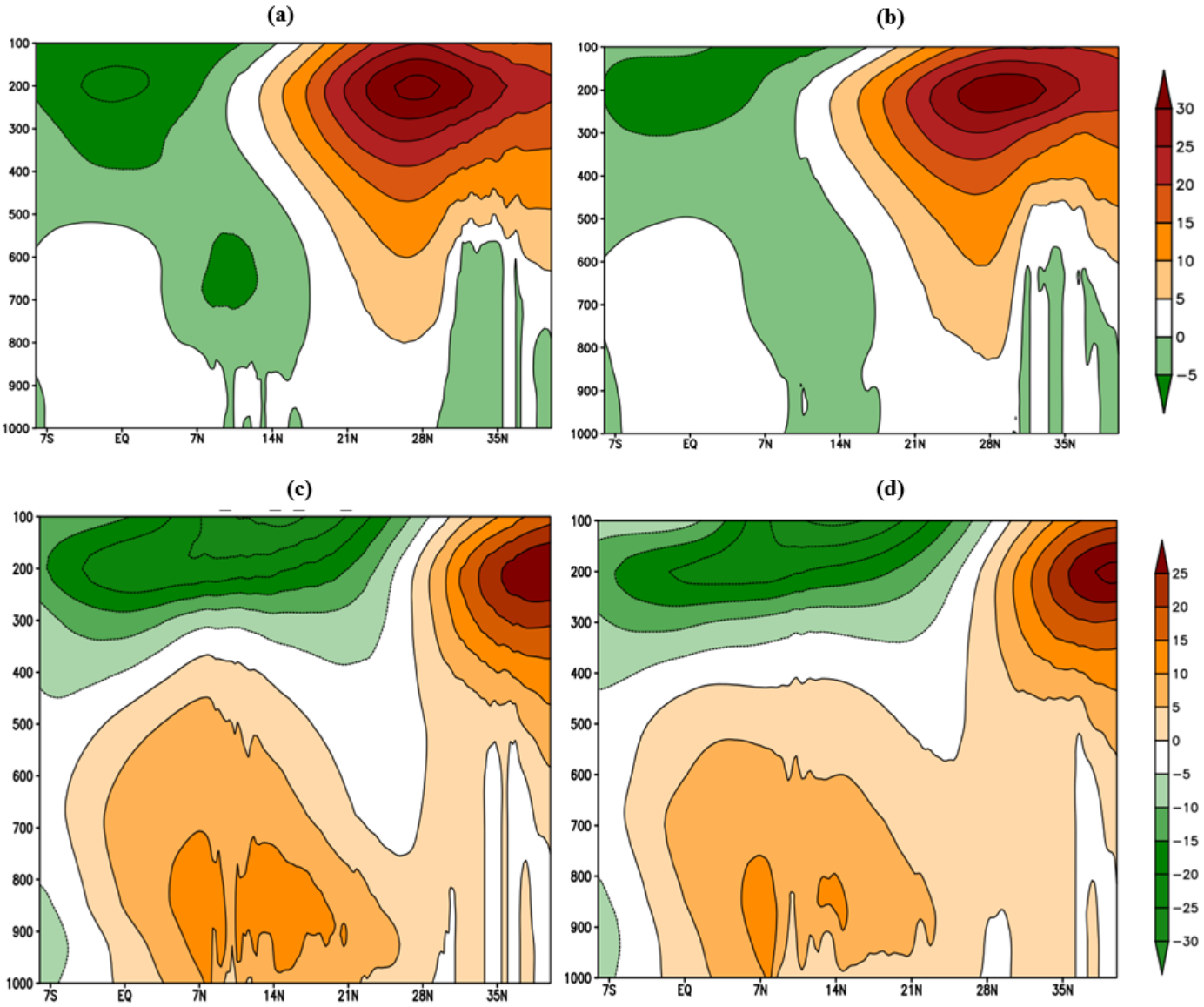

Figure 10

Latitude-height section of zonal winds along 78^0 E longitude corresponding to Pre-Monsoon (a) WRF, (b) ERA and summer monsoon (c) WRF, (d) ERA

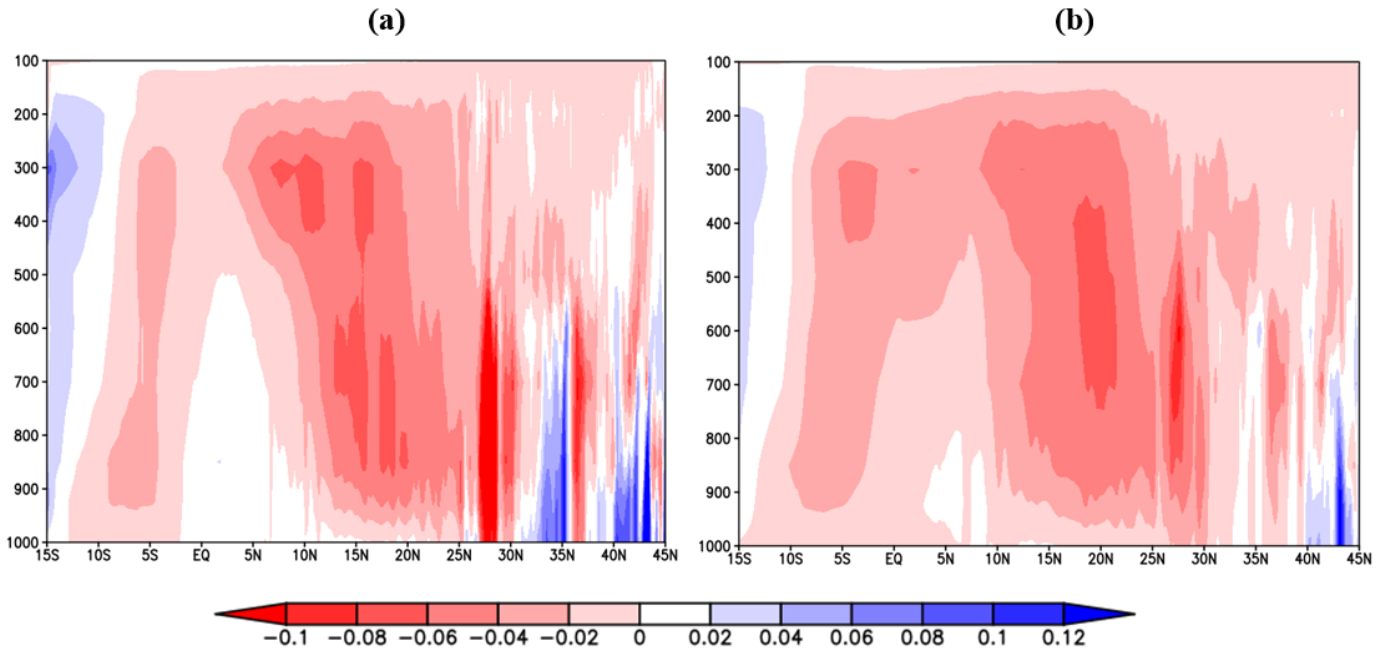

Figure 11

Latitude-pressure profile of ω (Pa/s) averaged over 65^0–95^0 E longitudes for the monsoon season for the period 2007-2021. (a) WRF, (b) ERA. By convention, the negative (positive) values represent rising (sinking) motion.

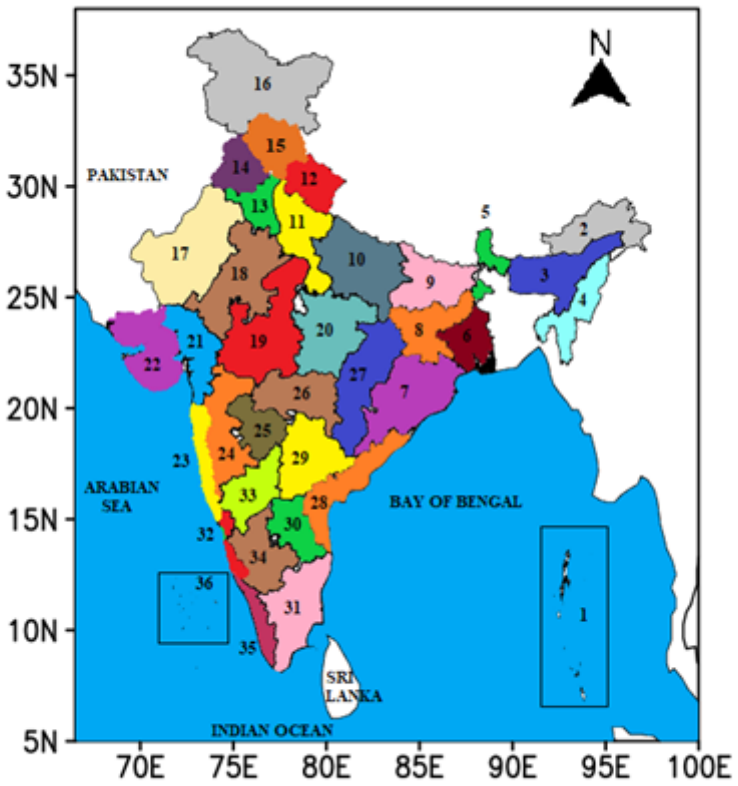

1	Andaman & Nicobar Islands	19	West Madhya Pradesh
2	Arunachal Pradesh	20	East Madhya Pradesh
3	Assam & Meghalaya	21	Gujarat
4	Nagaland,Manipur,Mizoram,Tripura (N.M.M.T)	22	Saurashtra & Kutch
5	West Bengal & Sikkim	23	Konkan & Goa
6	Gangetic West Bengal	24	Madhya Maharastra
7	Orissa	25	Marathwada
8	Jharkhand	26	Vidarbha
9	Bihar	27	Chhattisgarh
10	East Uttar Pradesh	28	Coastal Andhra Pradesh
11	West Uttar Pradesh	29	Telangana
12	Uttaranchal	30	Tamilnadu
13	Haryana	31	Rayalaseema
14	Punjab	32	Coastal Karnataka
15	Himachal Pradesh	33	North Interior Karnataka
16	Jammu & Kashmir	34	South Interior Karnataka
17	West Rajasthan	35	Kerala
18	East Rajasthan	36	Lakshadweep

Figure 12

The 36 Meteorological subdivisions of India.

Supplementary Files

This is a list of supplementary files associated with this preprint. Click to download.

- Appendix.docx